Master Level Thesis

European Solar Engineering School

No. 265, Sept. 2020

Techno Economic Analysis of Reverse Osmosis Combined with CSP + PV in Kuwait

Master thesis 30 credits, 2020
Solar Energy Engineering

Author:
Olof Eriksson

Supervisors:
Diego Alarcón
Patricia Palenzuela
Mats Rönnelid

Examiner:
Ewa Wäckelgård

Course Code: EG4001

Examination date: 2020-06-17

HÖGSKOLAN DALARNA

MASTER THESIS

Dalarna University
Solar Energy Engineering

Abstract

Seawater desalination plays an important role when fighting the freshwater scarcity that many places around the world are currently facing. The increasing need for desalinated water is followed by a high energy demand. It is therefore essential that an expansion of desalination capacity is accompanied by a parallel use of renewable energy sources in this process. This thesis presents a techno-economic study on a reverse osmosis (RO) desalination plant, with a nominal power consumption of 15 MW, that is powered by a concentrated solar power (CSP) plant combined with a photovoltaic (PV) power plant, in Kuwait. The main aim of this thesis was to find which system designs would give the lowest global warming potential and levelized cost of the desalinated water. In addition, it has been investigated how electricity price and emission allowance cost could make a solar power plant competitive to the grid. For this purpose, some components in the whole system were simulated using *System Advisor Model* and *Engineering Equation Solver*. With the results obtained from the simulations, a dynamic model of the whole system was developed in *MATLAB, Simulink* where simulations were done for a typical meteorological year in Shagaya, Kuwait. Both on-grid and off-grid systems were considered.

In the on-grid case, the lowest cost of water was obtained with only PV (ca 0.65 USD/m^3) and this could reduce carbon emissions by 30 % compared to only using the grid. Combining CSP and PV could reduce the carbon emissions by 85 % but with a 35 % increase in water cost. It was found that an electricity price of 0.1 USD/kWh or an emission allowance cost of 70 USD/$tCO_{2\text{-eq}}$ would make a CSP + PV plant competitive to the grid. These results indicate that the choice of which system is best for powering an on-grid RO plant depends on how the environmental and economic factors are prioritised. In the case of the off-grid system, both the lowest cost of water (ca 0.9 USD/m^3) and the highest capacity factor were obtained with a CSP + PV plant with 16 h of storage, a solar multiple of 3 and a PV capacity of 28 MW.

Acknowledgment

First, I would like to thank Diego Alarcón and Patricia Palenzuela at CIEMAT-PSA, who advised and supported me throughout the whole process. Even when Spain went under lockdown, due to COVID-19, and I had to return Sweden, they managed to provide the support I needed to see this though.

I would like to thank Mats Rönnelid at DU who took his time to answer my questions and discuss the project when I felt the need to.

Also, many thanks to the friends I made in Spain, who helped me with the language barriers and made my, unfortunately short, time in Almería unforgettable.

And of course, my family, my friends, and my girlfriend who have supported me and endured my absent mind these past few months.

Contents

Abbreviations

Abbreviation	Description
CF	Capacity Factor
CSP	Concentrated Solar Power
EF	Emission Factor
GWP	Global Warming Potential
LF	Load Fraction
LCOE	Levelized Cost of Electricity
LCOW	Levelized Cost of Water
O&M	Operation and Maintenance
PV	Photovoltaic
PB	Power Block
RO	Reverse Osmosis
SAM	System Advisor Model
SEC	Specific Energy Consumption
SF	Solar Field
SM	Solar Multiple
TES	Thermal Energy Storage

Nomenclature

Symbol	Description	Unit
A	Wetted area of the cold or the hot tank	m^2
C	Cost for the CSP, PV or RO plant	USD
c_p	Specific heat capacity	J/(kg °C)
E_{CSP}	Annual electric energy generated by the CSP plant	kWh
E_{PV}	Annual electric energy generated by the CSP plant	kWh
E_{tot}	Total annual electric energy generated	kWh
η_{th}	Thermal efficiency of the power block	-
m_{ct}	Mass content of molten salt in the cold tank	kg
m_{ht}	Mass content of molten salt in the hold tank	kg
$\dot{m}$	Mass flow rate of molten salt at point 1, 2, 3, or 4	kg/s
$O\&M$	Operation and maintenance cost	USD/year
P_{CSP}	Power generated by the CSP plant	kW
P_{goal}	Desired power output	kW
P_{PV}	Power generated by the PV plant	kW
P_{RO}	Power consumed by the RO plant	kW
P_{tot}	Total generated power	kW
Q_{ct}	Energy content in the cold tank	J
Q_{ht}	Energy content in the hot tank	J
$\dot{Q}_{\mathrm{Lct}}$	Thermal losses, cold tank	W
$\dot{Q}_{\mathrm{Lht}}$	Thermal losses, hot tank	W
$\dot{Q}_{\mathrm{SF}}$	Thermal power received from the SF	W
$\dot{Q}_{\mathrm{PB}}$	Thermal power consumed by the PB	W
ρ	Density of the molten salt	kg/m^3
T	Temperature of the molten salt at point 1, 2, 3, or 4	°C
T_{amb}	Ambient air temperature	°C
T_{cond}	Condensation temperature	°C
u	Wetted loss coefficient	$W(m^2\ °C)$
V_{water}	Annual production of water	m^3

1 Introduction

As the world slowly but steadily gets warmer and the human population increases, we are faced with new challenges when it comes to ensure the survival and health of our fellow earthlings. Both in the present and in the future. The higher temperature leads to an increased displacement of water i.e. more droughts and more floods, both which can be very damaging to freshwater reserves. In addition, the growing population increases the demand for freshwater, which is not only used for drinking and washing. Without freshwater there is no food, no clothes, paper etc. There are few (if any) anthropogenic processes that do not (directly or indirectly) rely on freshwater. One may think that this should not be a problem when living on the so called "blue planet" known as Earth. But today, more than 2.3 billion people are living in water scarce areas [1] and only 2.5 % of all water in the world is freshwater. Around 30 % of that fresh water is ground water, 69 % is frozen and 1 % is in lakes, rivers, wet areas and the atmosphere [2]. So, only about 0.026 % of all the blue covering about 70 % [2] of the Earth's surface is freshwater and the rest is seawater. This makes desalination of seawater a good candidate to counter water scarcity in many affected areas.

Following the growing production of desalinated water comes an increased energy need. Seawater desalination is a quite energy intensive process, whether it is thermal or mechanical. This makes it imperative that the energy used comes from renewable sources, to avoid any further escalation of the problems caused by global warming.

Solar energy could be ideal for this application, since dry areas tend to have high levels of solar radiation. But the intermittent production from solar energy technologies, like photovoltaics (PV), could affect the operation of a desalination plant. It is therefore essential to find solutions that provide a high dispatchability, which could be archived by combining different renewable power generation technologies and energy storage technologies. This study proposes a hybrid system composed of a PV plant and a concentrated solar power (CSP) plant that provides electricity to a reverse osmosis (RO) desalination plant. Since the bigger developments within the desalination market will take place in the Middle East region during the next years [3], a location in a Gulf country (Kuwait) has been selected for the present study

1.1 Aims

The main aim of this work is to do a techno-economic study of a 15 MW solar desalination system with CSP + PV + RO in Kuwait. Two systems have been considered for this study: an on-grid system (system 1) and a standalone system (system 2). Simulations have been done for a typical meteorological year in Shagaya, Kuwait. Specific objectives are:

- Conduct a parametric study to find the optimal designs regarding levelized cost of energy (LCOE), the levelized cost of water (LCOW) and global warming potential (GWP) of the produced water.

- Investigate how the energy price and emission penalties may motivate a higher solar fraction in the energy mix.

1.2 Method

The methodology of the project has been structured as follows:

1. Literature review: A literature review have been done in order to find research works related to the scope of this work and to justify the contribution of this thesis work. Some points to cover in the literature review are how CSP and PV can be coupled, if there are other studies on RO plants, or other desalination technologies, with PV and/or CSP and what problems or limitations these types of systems may have.

2. Modelling and simulations: Based on knowledge acquired from literature review, decide on one or several systems with different operation strategies. The software used for modelling and simulating the system have been *MATLAB, Simulink*, *System Advisor Model (SAM), Engineering Equation Solver (EES)* and *Excel*. Simulating some part systems in *SAM* and *EES* and letting them interact with each other through *Simulink* was a way to overcome some difficulties in modelling while making the simulation process more efficient. A 1 MW PV array was designed and simulated in *SAM* and the hourly net power output from the PV plant was then exported into *MATLAB,* to be used in the *Simulink* model. The CSP plant was simulated in both *SAM* and *Simulink,* where the solar field (SF) was simulated and designed in *SAM* to utilize its optimizing tool for heliostat field and receiver tower. The hourly thermal output from the SF and the receiver efficiency was then extracted to be used as inputs in the *Simulink* model. The power block (PB) was simulated in an *EES* model developed by CIEMAT-PSA, from where two equations were obtained to determine the varying efficiency of the PB. These equations were then used in the PB model in *Simulink*. The model of the thermal energy storage (TES) and the RO have been developed in *Simulink,* where all parts of the whole system interacts according to several control functions. The *Simulink* model then gives all necessary outputs for analysing the performance of the whole system in *Excel*.

3. Parametric study: A parametric study of the main components (PV plant, TES and SF) has been done in terms of size using above mentioned simulation tools. The size of the PV plant is defined by the peak power production of the PV modules at standard test conditions (solar irradiation of 1000 W/m^2 and cell temperature of 25 °C) and is expressed in MW. The TES size is defined by how many hours the PB can operate at 100 % capacity. The size of the SF is defined by the solar multiple (SM), which is the ratio between the thermal power output of the SF during design conditions and the thermal power required for the PB to operate at nominal capacity. First a parametric study was done for the CSP plant regarding LCOE by changing the solar multiple (SM) and hours of storage. The parametric study of system 1 was done with regards to solar fraction, LCOE, LCOW and GWP by varying SM, TES and PV size. It has also been investigated how the electricity price and carbon emission penalties affects the optimal system design regarding LCOW. In case of system 2, an additional parameter has been varied apart from the already mentioned, that is the number of trains in the RO plant for different CSP + PV configurations. This has only been analysed with regards to LCOW and capacity factor (CF), due to system 2 being 100 % solar powered. The capacity factor is the ratio of energy generated over a year divided by the installed capacity.

1.3 Previous Work

Many studies have been carried out on solar driven desalination systems, though few of them on CSP + PV with desalination. This section presents some previous studies on CSP + PV and solar driven desalination.

1.3.1. CSP + PV

The decreasing price for PV that has been seen in the last years has made PV preferable to CSP regarding direct power generation. CSP's biggest strength is that it is dispatchable when it is coupled with a TES, and can deliver a steady power output even when there is no solar irradiation [4]. The cheaper power from PV combined with the dispatchability of CSP could then reduce the costs for CSP while keeping a high dispatchability and a high CF. According to a study where an optimisation of a hybrid CSP + PV plant was done for two different locations, Ottana (Italy) and Ouarzazate (Morocco), it is most cost effective to use CSP + PV if a constant power output is required for more than 16 h. If only 8 h is needed, then a PV + battery system would be better [5].

In a study carried out by Platzer [6] it was revealed how the combination of a 50 MW PV plant and a 50 MW CSP plant may enhance the dispatchability and reduce the size of the SF needed in the CSP plant. In this case, the cheaper electricity generated from the PV plant is prioritized during the day which allows the thermal energy from the SF to be stored and used to generate electricity during night-time. Furthermore, the LCOE was reduced from 0.152 €/kWh to 0.124 €/kWh by combining CSP with PV compared to having only CSP [6]. Another study done, with location data from Atacama Desert in Chile, investigated how the CF could be improved when a CSP plant is combined with a PV plant. It showed that the CF could be increased from 80 % to 90 %. Also, it was found that that it is favourable to optimize the tilt of the PV panels for winter conditions to reduce seasonal variations, which turned out to be important when designing plants with high CF [4].

Zurita et al. [7] conducted a techno-economic evaluation of a CSP + PV system with molten salt TES and Li-ion battery storage. The system was supposed to deliver a constant power of 100 MW for 24 h a day. As in previous cases, the operation of the PV plant was prioritised during the day and the CSP plant and batteries acted as buffer. The CSP plant was set to run on minimum capacity (30 %) when the production from the PV plant exceeds 65 MW and turn off when it exceeds 95 MW with the aim to reduce the shutdown sequences of the PB in the CSP plant. Also, it was established that the excess power from the PV plant would be stored in the battery system during these operation modes or dumped if the batteries are full, and the batteries would discharge when the TES cannot meet the demand. The results from this study showed that the lowest LCOE (77.2 USD/MWh) was obtained when using 14 h TES, a SM of 2.2, 130 MW PV and no battery storage. However, the highest CF (90.3 % compared to 82.2 % in previous) was reached with 14 h TES, SM 2, 190 MW PV and 400 MWh of battery storage. In this case the LCOE was 87.5 USD/MWh. According to this study a cost reduction of 90 % for the battery storage would be needed for a hybrid system with batteries to reach an LCOE as low as one without batteries.

1.3.2. CSP and/or PV with Desalination

In a techno-economic study carried out by Laissaoui et al. [8], a comparison was done between stand-alone CSP + RO and PV + RO systems. In this study, CSP plants both with and without TES were considered, while the PV plant was not coupled with any storage. Two operation scenarios were considered: whole unit, which had two operation strategies, and gradual capacity. Where the "whole unit" scenario considers a single unit (train) for the entire RO plant that operates within a safe range, according to power availability (strategy 1). If the available power goes below the safe range, the water quality is ensured by turning off some pressure vessels of the RO unit gradually (strategy 2). Here the production of water changes with the number of active pressure vessels and it was assumed that the pump operates at 80 % efficiency in the whole range. The "gradual capacity" scenario uses multiple subunits (trains) that can shut on and off gradually depending on power availability and all of them run at nominal power (i.e. cascading). Three RO systems were considered in the simulations, one without any energy recovery device and two with different energy recovery devices: Pelton turbine with generator and pressure exchanger. The study showed that operation of the RO plant as a whole unit always had a higher water production than the gradual capacity operation. A PV powered RO unit without energy recovery was found to have increased water production from 12,229 m^3/day to 14,758 m^3/day when using proposed strategies for the whole unit scenario. Using CSP with TES proved to increase the water production significantly compared to CSP without any storage, obtaining an increase higher than 35000 m^3/day when using 14 h storage. The solution with the lowest LCOE was a CSP plant with 14 h storage and a RO plant with pressure exchangers. The price of the produced water was then 0.85 USD/m^3, which is low enough to compete with RO powered by fossil fuels, which can range between 0.6 – 1.9 EUR/m^2 [8].

Valenzuela et al. [9] did a study on cogeneration of electricity and water using a CSP + PV plant and a multi-effect distillation (MED) unit in northern Chile. In the considered system the MED is driven by exhaust steam from the CSP plant and it is connected in parallel with

the condenser of the PB. The CSP plant is controlled to prioritise the power output from the PV plant, so that both plants deliver a total power of 100 MW. In this case the MED only functions when the electrical power output from the CSP plant exceeds 50 MW. Otherwise all excess heat from the CSP is dumped through the condenser. With this operation strategy, a high production from the PV plant will lead to a penalty in water production, due to the CSP running more hours on partial capacity. It was found that the longest operating hours for the MED plant were reached with a nominal PV capacity of 60 MW electric and the longest operating hours for delivering power were achieved with 100 MW PV. Hybridisation with CSP + PV + MED resulted in a 7.6 % reduction of CF and an increase of 12.7 % in LCOE compared to CSP + PV. The lowest LCOW was obtained there were no PV plant included in the system and the lowest LCOE was reached with PV size of 100 MW [9].

As far as the author knows, there are no studies on CSP + PV + RO systems in the scientific literature. This thesis work presents a techno-economic analysis considering the implementation of such a system in Kuwait.

1.4 Theoretical Background

There are three main technologies for large scale seawater desalination: multi-stage flash (MSF), MED and RO. This part briefly goes into the theory of the first two while explaining RO with a bit more depth. The very basics regarding CSP central receiver systems with molten salt thermal storage are also covered.

1.4.1. Multi-Stage Flash

MSF is a thermal distillation process where vapour is generated by flash evaporation when saline water enters a chamber (stage) where pressure is below its saturation point. As the water evaporates, the temperature of the water falls along with the saturation pressure. The evaporation stops when the saturation pressure and the pressure in the stage are at equilibrium. Evaporated water is condensed when it reaches a heat exchanger, where it discharges latent heat to preheat seawater or brine. Condensed water is collected and exits the system as fresh water. The water which do not evaporate is led to the next stage which has a lower pressure and the same process is repeated. A part of the cooling water is used as feed water and is preheated in each stage before it is heated in the heater and fed to the first stage. This process is illustrated in Figure 1.1. To create and maintain the pressure in the stages a vacuum system is used. This also removes non-condensable gases that are released from the seawater, which are a problem since they raise the pressure in the stages and reduce the heat transfer to the heat exchangers. MSF systems can withstand quite harsh conditions and is thus very suitable for water with very high salinity, pollution and/or temperature [10].

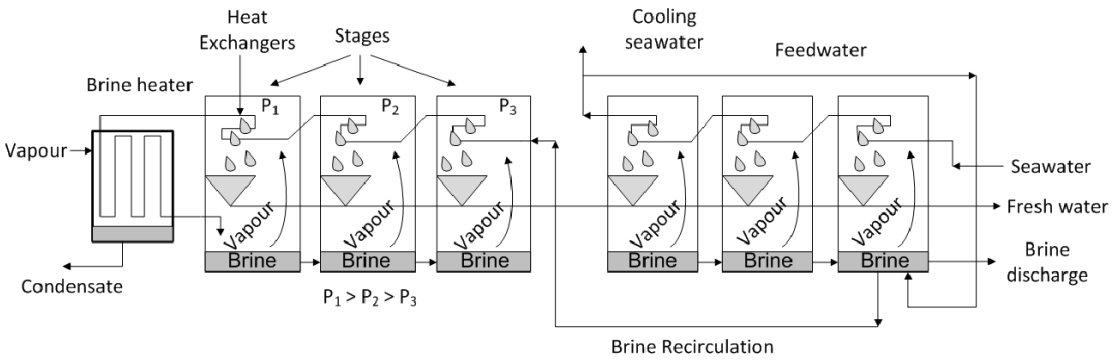

Figure 1.1Illustration of the process in a MSF plant [11] (with permission from P. Palenzuela).

1.4.2. Multi-Effect Distillation

As for MSF, MED is a thermal distillation process that uses multiple stages at decreasing pressures. In the first stage, an external energy source (steam or liquid) is used to drive the distillation process. Seawater is evaporated when it is sprayed over the evaporator tubes. The

generated vapour goes through a demister and then to the following evaporator located in the next stage. The brine also goes to the next stage, that is at a lower pressure, which leads to evaporation of part of the brine by flash. In this stage, un-evaporated brine from the previous effect is sprayed over the tubes of the evaporator and the vapour coming from the previous effect condenses as it releases its latent heat of condensation. A part of the generated vapour in one evaporator can be led through a preheater to preheat the seawater before it enters the following evaporator. This is done to increase the thermal efficiency of the process. The same process is repeated in the following stages until the last one, where all vapour goes to a condenser that preheats seawater (used as a cooling source) and the remaining vapour. The resulting brine from the last stage is finally discharged. Figure 1.2 illustrates the described processes. MED plants can improve their thermal efficiency by the use of steam ejectors (thermal vapour compression) or absorption heat pumps [10].

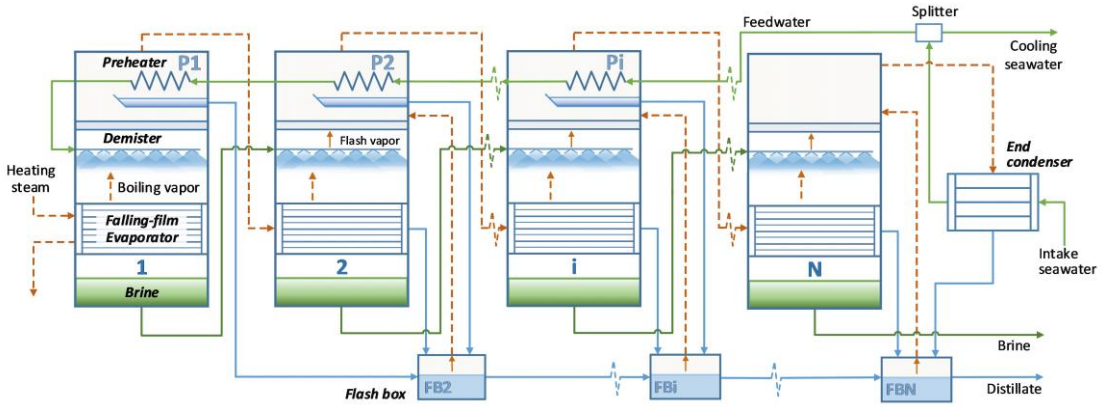

Figure 1.2 Illustration of the process in a MED plant [11], (with permission from P. Palenzuela).

1.4.3. Reverse Osmosis

Compared to the previously mentioned technologies that mainly use thermal energy, reverse osmosis is a mechanical energy-driven desalination technology. In the RO process water is filtered through membranes using high pressure to remove salts, large molecules, bacteria and pathogens. Clean water (permeate) passes through the membrane while salts and other molecules are stopped and eventually rejected as brine (concentrate). The need for a high pressure is mainly to overcome the osmotic pressure. The osmotic pressure is defined as the pressure needed to overcome the natural osmosis, as illustrated in Figure 1.3 [12].

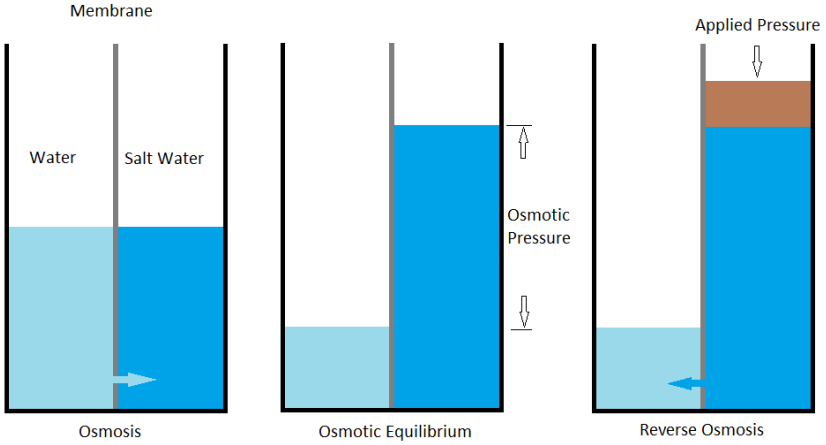

Figure 1.3 Figure showing the principle of reverse osmosis, reprinted from [12].

A seawater RO plant can be designed in different configurations to improve the water quality and reduce the specific energy consumption (SEC): using multiple passes, stages or energy recovery devices. In a RO system with multiple passes the seawater is filtered more than one time which improves the quality of the water. Multiple pass systems are more expensive than single pass ones and have a lower production. They are generally used under certain conditions when a single pass system cannot guarantee a desired water quality. The use of two passes instead of one also reduce the feed pressure to the first pass thus improving the

operation of the RO system, by reducing the need for cleaning the membranes and the overall feed RO pressure. However, it is important to note that they require an extra pump to boost the pressure between the first and the second pass [12]. A double pass system is illustrated in Figure 1.4

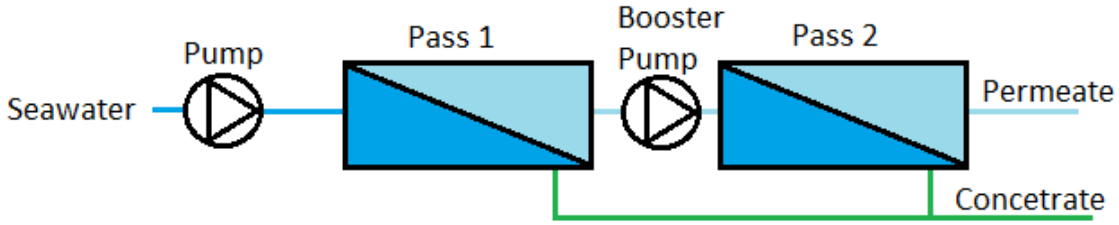

Figure 1.4 Double pass RO system, reprinted from [12].

To improve the water recovery of the system the concentrate can be treated separately in another stage. A RO system with two stages is presented in Figure 1.5.

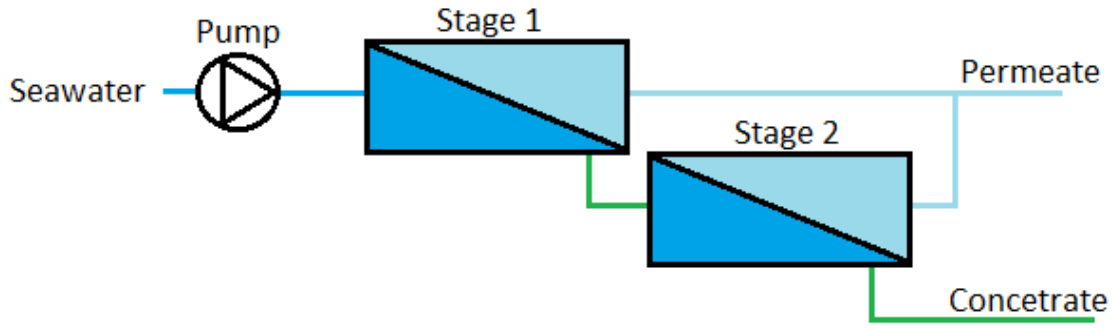

Figure 1.5 Double stage RO system, reprinted from [12].

On the other hand, the SEC of the RO systems can be reduced using an Energy Recovery Device. This device recovers a part of the energy content in the high-pressured concentrate. There are many types of energy recovery devices available, but the Pelton turbine with generator or the pressure exchanger are the most common alternatives, being the pressure exchanger is the most efficient one [8] [12]. Using a pressure exchanger, the pressure of the reject brine is transferred to a portion of the feed water with an efficiency exceeding 97 % [13]. This pressurised water is returned to the main feed water stream before entering the membranes, as shown in Figure 1.6. This reduces the flow through the main high-pressure pump significantly, which reduces the energy consumption. An extra booster pump is needed between the PEX and the main feed water stream to overcome the small pressure difference between the two water flows [13].

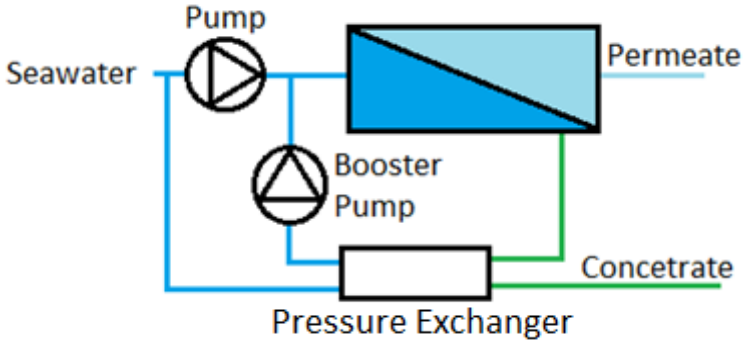

Figure 1.6 Single stage/pass RO system with pressure exchanger, reprinted from [12].

However, there are some problems associated with seawater RO plants. Not all compounds are removed by the membranes and further treatment is needed to remove neutrally charged compounds like boron and N-nitrosodimethylamine. It is also necessary to add minerals to the permeate since it is lacking of essential minerals which makes it inappropriate for human consumption and corrosive to the water distribution system [12].

Another important problem associated with RO, and other desalination technologies, is the environmental concern regarding the rejected brine management. The reject brine does not only contain salt from the seawater, it can also contain various chemicals and sludge from the pre-treatment. The impact of these can be reduced with the right post treatment. Without a good dispersal of the brine, the high density brine can sink to the seafloor and kill plants and other organisms that live on the seafloor [12].

1.4.4. Concentrated Solar Power

The type of concentrated solar power technology considered in this study is a central receiver tower with molten salt storage. It consists of four main subsystems: heliostat solar field, receiver tower, storage system and a power block.

The heliostats are mirrors that use two axes tracking to follow the sun and to reflect the sunrays to a receiver placed in a tower. In the receiver, a fluid is heated (in this case molten salt) up to the desired temperature and can then be stored as sensible heat for later use or used directly to drive a steam-based power cycle. The thermal storage system consists of two tanks, hot and cold, which are charged and discharged as explained hereinafter. In the charging process, molten salt is taken from the cold tank and heated in the receiver to then be stored in the hot tank. In the discharging process, molten salt is taken from the hot tank and cools down as it discharges thermal energy to generate superheated steam in the steam-generator of the power block. The cold salt is then stored in the cold tank. The common composition of salts for this application, called solar salt, is made up of 60 % $NaNO_3$ and 40 % KNO_3 and has a melting point at 220 °C and allow operating temperatures up to 585 °C [14].

2 Description of System

Two main systems have been compared: an on-grid system (system 1) and an off-grid system (system 2). For both systems, a techno-economic analysis of a RO unit powered by a CSP plant and/or by a PV plant has been carried out. In the case of system 1, the grid can be used either as a backup or as the main power supply. This system considers in turn two cases: one where all surplus power is delivered to the grid (case a) and one where all surplus power must be discarded (case b). The last case tries to cover the uncertainty regarding the power limitations in the grid which may have implications in the analysis of LCOE, LCOW and GWP.

The whole energy system is designed to deliver 15 MW electrical, which is the power required by the considered RO plant at nominal conditions. The operation of the PV plant is always prioritized, so that the CSP plant can reduce its power output and store thermal energy while the PV plant is generating power. This increases the operation time and reduces the power fluctuation caused by the intermittent nature of the PV plant. A sketch of the whole system is presented in Figure 2.1.

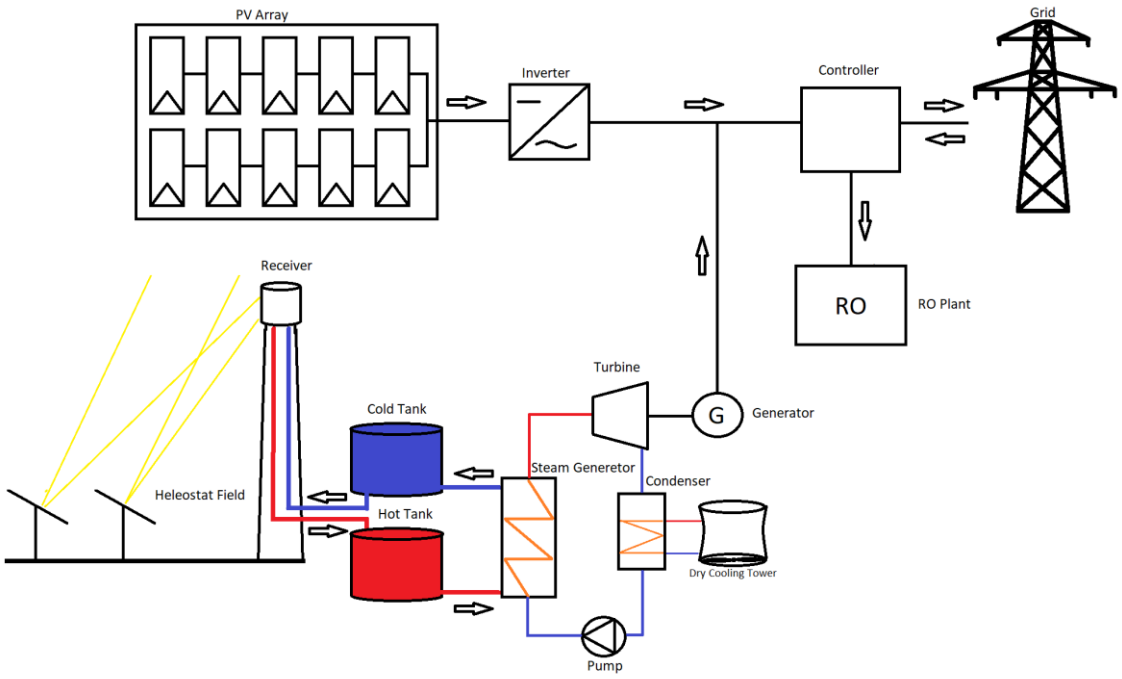

Figure 2.1 General sketch of an on-grid CSP + PV + RO system.

2.1 CSP Plant

The CSP plant is a central receiver tower system with a molten salt TES system. The molten salt is stored in two tanks: one cold, at 290 °C, and one hot, at 575 °C. The PB is air cooled and operates at 165 bar and 565 °C. It has an operating range of 30 – 100 % of the nominal power production (15 MW electric). It is assumed that 15 % extra power must be generated to cover the parasitic loads of the CSP plant. This gives a total gross capacity of 17.25 MW electric. The design thermal efficiency is 40 % and the design thermal power is 43 MW thermal, which is what the SF is designed to deliver considering a SM of 1.

2.2 PV Plant

The inverter and the PV modules have been selected from *SAM*s' library. PV modules used are SPR-X20-445-COM by *SunPower*. These are 445 W DC modules with mono-crystalline silicon cells that have a degradation rate of 0.25 percentage points per year and a lifetime of 25 years [15]. The modules are oriented to the south, with a fixed tilt of 29° (same as the latitude of Shagaya) and a ground coverage ratio of 30 %. The inverters used are 1 MW AC

inverters manufactured by *Sungrow Power Supply Co* called SG1000MX. One PV array with the size of 1 MW DC at standard test conditions consists of 2,248 PV modules and a single inverter.

2.3 RO Plant

The RO plant considered in system 1 is a single train RO unit that always operates at nominal power (15 MW electric). It is assumed to have an availability of 95 % and a SEC of 4 kWh/m^3 [16]. The RO plant considered in system 2 uses one or multiple trains that operates binary (on/off) to match the available power. SEC and maximum availability are assumed to be the same as for system 1.

3 Model and Calculations

This section gives a description of the models and equations used when simulating and analysing the system.

3.1 Boundary Conditions

Simulations of the CSP + PV plant have been done using hourly average values of dry bulb temperature, direct normal irradiance, and global horizontal irradiance for a typical meteorological year for Shagaya, Kuwait. Weather files were obtained from the European Commission's Photovoltaic Geographical Information System [17]. Annual average values are presented in Table 3.1. The salinity of the seawater is assumed to be 45000 mg/l.

Table 3.1 Yearly average meteorological values [17].

Parameter	*Value*	*Unit*
Global horizontal irradiation	2170	kWh/(m^2 year)
Direct normal irradiation	2210	kWh/(m^2 year)
Ambient temperature	24.8	°C

3.2 CSP Plant

The whole CSP system was simulated in *Simulink* together with the RO and the PV plant, except the SF which was simulated in *SAM* and then imported to the *Simulink* model.

3.2.1. Power Block

For simplicity, two polynomial expressions were used to calculate the efficiency of the PB. These equations were obtained by running simulations at different conditions using a model implemented in *EES*, provided by CIEMAT-PSA. The thermal efficiency (η_{th}) of the PB was calculated by Equation 3.1, as a function of the condensation temperature (T_{cond}). The efficiency fraction (EF), which is defined as the ratio between the thermal efficiency at full load and at part load, was calculated by Equation 3.2 as a function of the load fraction (LF). LF is defined as the ratio between power generated and the nominal power.

$$\eta_{th} = -0.001243 \cdot T_{cond} + 0.4719 \qquad \textit{Equation 3.1}$$

This polynomial equation has been obtained from the values presented in Table 3.2 with a root mean square error of 0.00029.

Table 3.2 Table showing η_{th} in relation to T_{cond}.

T_{cond} (°C)	η_{th}
40	0.422
45	0.416
50	0.410
55	0.404
60	0.397
65	0.391
70	0.384

$$EF = -0.4774 \cdot LF^3 + 0.8606 \cdot LF^2 - 0.2437 \cdot LF + 0.8596 \qquad \textit{Equation 3.2}$$

This polynomial equation has been obtained from the values presented in Table 3.3 with a root mean square error of 0.0028.

Table 3.3 Table showing EF in relation to LF.

LF	*EF*
1	1.00
0.9	0.99
0.8	0.97
0.7	0.95
0.6	0.91
0.5	0.88
0.4	0.87
0.3	0.86

3.2.2. Solar Field

A CSP system with 24 h TES and a SM of 1 was simulated in order to obtain an output from the SF, independent of the TES and the PB. The oversizing of the storage is to ensure that the receiver can utilize all energy captured by the SF, i.e. without defocusing any heliostats. If the storage would be small then there is a risk that it could be full at some time steps, forcing the SF to reduce its output according to the control functions in *SAM*. With no manipulation in the operation of the SF it can be assumed that the SF can be viewed as an independent system. The inputs used in *SAM* are presented in Table 3.4, other inputs were set to default.

Table 3.4 Input values for SAM.

Input	*Value*	*Unit*
Design turbine gross output	17.25	MW
Estimated gross to net conversion factor	0.87	-
Design thermal efficiency	0.4	-
Design point DNI	900	W/m^2
Solar multiple	1	-
HTF hot temperature	575	°C
HTF cold temperature	290	°C
Full load hours of storage	24	h

Hourly values of the incident irradiance on the receiver and receiver efficiency were then imported to *MATLAB* and used in the *Simulink* model. The size of the solar field could there be changed by multiplying the receiver output by the desired SM. The design thermal power ($\dot{Q}_{design}$) that has to be delivered to the PB at nominal power is calculated by Equation 3.3, which is in turn used to determine the size of the SF and the storage.

$$\dot{Q}_{design} = \frac{P_{\mathrm{CSP}_{\mathrm{design}}} \cdot 1.15}{\eta_{\mathrm{th}_{\mathrm{design}}}} \qquad \textit{Equation 3.3}$$

Where $P_{\mathrm{CSP}_{\mathrm{design}}}$ is the CSP plant's nominal electrical power output (kW), $\eta_{\mathrm{th}_{\mathrm{design}}}$ is the design thermal efficiency and 1.15 is the extra power needed to cover the parasitic loads.

3.2.3. Thermal Energy Storage System

In the case of the TES, the two tanks have been simulated separately. Four main points are considered in the model: 1 (between receiver and hot tank), 2 (between hot tank and PB), 3 (between PB and cold tank) and 4 (between cold tank and receiver). It has been assumed that the temperature in point 2 (T_2) is the same as the temperature in the hot tank and T_4 the same as the temperature in the cold tank. Temperatures T_1 and T_3 have been assumed

to be constant at 575 °C and 290 °C respectively. The energy content in the hot and the cold tank (Q_{ht} & Q_{ct}, respectively) is determined from the energy balances presented in Equation 3.4 and Equation 3.5.

$$Q_{\mathrm{ht}} = \int (\dot{m}_1 c_{p1} T_1 - \dot{m}_2 c_{p2} T_2 - \dot{Q}_{\mathrm{Lht}}) dt \qquad \textit{Equation 3.4}$$

$$Q_{\mathrm{ct}} = \int (\dot{m}_2 c_{p3} T_3 - \dot{m}_1 c_{p4} T_4 - \dot{Q}_{\mathrm{Lct}}) dt \qquad \textit{Equation 3.5}$$

Where $\dot{m}_1$ and $\dot{m}_2$ are the mass flow rates of the molten salt during charge and discharge (kg/s), c_p is the specific heat capacity of the molten salt (J/(kg °C)) and $\dot{Q}_{\mathrm{L}}$ is the thermal loss from the tank.

The molten salt content in the tanks in terms of mass (m_{ht} & m_{ct}) is calculated by Equation 3.6 and Equation 3.7.

$$m_{\mathrm{ht}} = \int (\dot{m}_1 - \dot{m}_2) dt \qquad \textit{Equation 3.6}$$

$$m_{\mathrm{ct}} = \int (\dot{m}_2 - \dot{m}_1) dt \qquad \textit{Equation 3.7}$$

$\dot{m}_1$ and $\dot{m}_2$ are determined from Equation 3.8 and Equation 3.9.

$$\dot{m}_1 = \frac{\dot{Q}_{\mathrm{SF}}}{c_{p1} T_1 - c_{p4} T_4} \qquad \textit{Equation 3.8}$$

$$\dot{m}_2 = \frac{\dot{Q}_{\mathrm{PB}}}{c_{p2} T_2 - c_{p3} T_3} \qquad \textit{Equation 3.9}$$

Where $\dot{Q}_{\mathrm{SF}}$ is the heat delivered by the SF through the receiver (W) and $\dot{Q}_{\mathrm{PB}}$ is the heat delivered to the PB (W).

c_p is calculated by Equation 3.10, which is the relation between c_p and T (in °C) obtained by Zavoico [18], and $\dot{Q}_{\mathrm{PB}}$ is defined by Equation 3.11.

$$c_p = 1443 + 0.174 \cdot T \qquad \textit{Equation 3.10}$$

$$\dot{Q}_{\mathrm{PB}} = \frac{P_{\mathrm{CSP}} \cdot 1.15}{\eta_{\mathrm{th}} \cdot EF} \qquad \textit{Equation 3.11}$$

Where P_{CSP} is the power delivered by the CSP plant (W) and 1.15 is the extra power needed for the parasitic loads.

Thermal losses in the tanks ($\dot{Q}_{\mathrm{Lht}}$ & $\dot{Q}_{\mathrm{Lct}}$) are accounted for and calculated by Equation 3.12.

$$\dot{Q}_{\mathrm{L}} = uA(T - T_{\mathrm{amb}}) \qquad \textit{Equation 3.12}$$

Where u is the wetted loss coefficient that applies to the part of the tank that is covered by the molten salt. A is the area of the tank shell that holds the molten salt (wetted area) and it is calculated by Equation 3.13. T is the temperature of the molten salt in the tank and T_{amb}

is the temperature of the ambient air surrounding the tank (°C). As a strong simplification, only the heat transfer through the tank wall between the molten salt and the ambient air is considered. This is based on the TES model in *SAM*. The wetted loss coefficient is assumed to be 0.4 W/(m^2 °C), which is the default setting in *SAM*.

$$A = \frac{4 \cdot m}{\rho \cdot d} \qquad \textit{Equation 3.13}$$

Where d is the diameter of the tank, which is set to 20 m, and ρ is the density of the molten salt (kg/m^3).

The temperature in each tank is determined by Equation 3.14.

$$T = \frac{Q}{mc_p} \qquad \textit{Equation 3.14}$$

The density of the molten salt is calculated by Equation 3.15, which is the relation between ρ and T (in °C) obtained by Zavoico [18].

$$\rho = 2090 - 0.636 \times T \qquad \textit{Equation 3.15}$$

Electrical power for pumping from the cold to the hot tank is calculated by Equation 3.16. The efficiency is assumed to be 85 %. It has been assumed that the power for pumping molten salt from the hot to the cold tank (P_{pump}) is accounted for in the parasitic loads of the PB.

$$P_{\text{pump}} = \frac{\dot{m}_1 g h}{\eta} \qquad \textit{Equation 3.16}$$

Where g is the gravitational acceleration (m/s^2), h is the height of the receiver tower (m) and η is the efficiency of the pump.

3.2.4. Controls

The CSP plant is designed to fill the gap between the PV output (P_{PV}) and the desired power output of 15 MW electric (P_{goal}) for the RO plant. The power load that the CSP plant must cover ($P_{l_{CSP}}$) is defined by Equation 3.17, with the limitation that it cannot operate below 30 % of its rated power ($P_{CSP\text{-}min}$). If $P_{l_{CSP}}$ goes below 30 % of P_{goal}, then the CSP plant will deliver $P_{CSP\text{-}min}$. If P_{PV} exceeds P_{goal}, then the PB is turned off. The simulated operation of the CSP and PV plants, for a day when above mentioned operation modes occur, is presented in Figure 3.1.

$$P_{l_{\text{CSP}}} = P_{\text{goal}} - P_{\text{PV}} \qquad \textit{Equation 3.17}$$

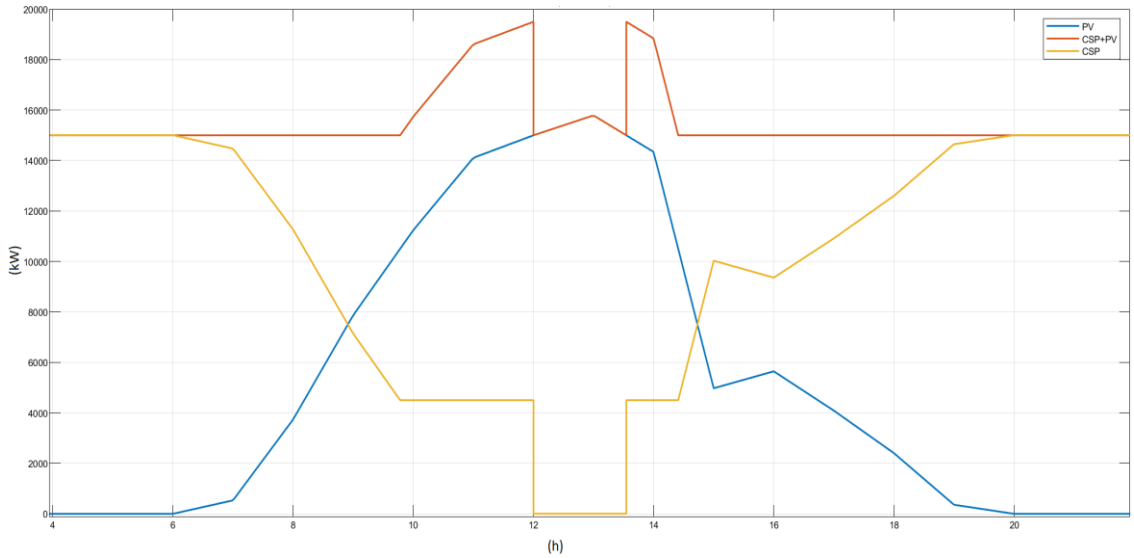

Figure 3.1 Diagram exported from Simulink, showing the simulated power output from the CSP and PV (individual and summarised) for one day. The simulated system has a SM of 3, 14 h TES and 20 MW of PV. Blue line is PV, orange is CSP + PV and yellow is CSP.

To avoid deep discharging, the PB turns off if the state of charge in the hot tank falls to 2 % and turns on again as it reaches 5 %. A similar approach is applied to avoid overcharging. If the state of charge in the cold tank falls to 2 %, and $\dot{Q}_{PB} < \dot{Q}_{SF}$, then the heliostat solar field is defocused to match the discharge ($\dot{Q}_{PB} = \dot{Q}_{SF}$). If $\dot{Q}_{PB} \geq \dot{Q}_{SF}$, then the SF operates without intervention. The complete flowchart of the control loops established in the CSP model is presented in Figure 3.2.

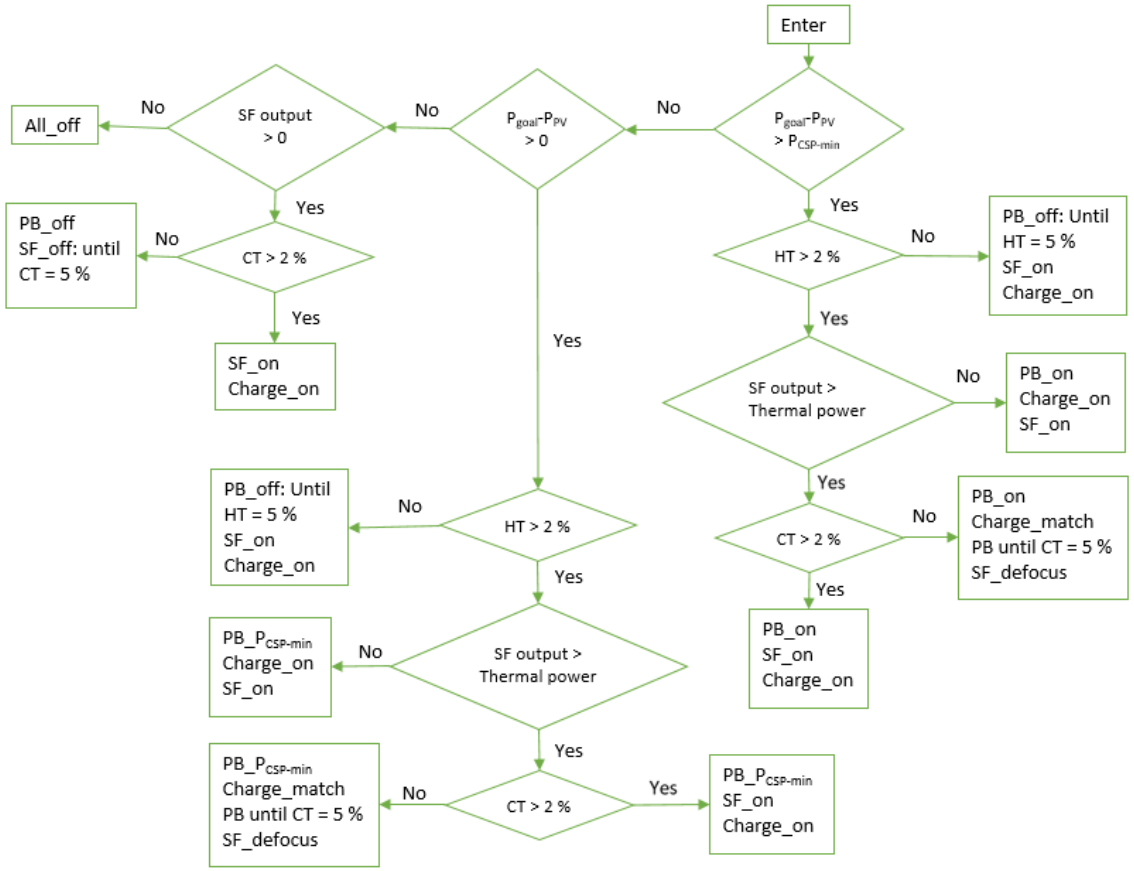

Figure 3.2 Flowchart of the control loops established in the CSP model. CT is the state of charge in the cold tank and HT is the state of charge in the hot tank.

3.3 PV Plant

A PV array with a rated DC power of 1 MW and one central inverter was designed and simulated in SAM. The hourly AC output was then imported to *MATLAB* and used in the *Simulink* model. The size of the PV plant was changed in *Simulink* by multiplying the AC output by the desired number of arrays to be used in the complete system.

As mentioned in section 2.2, the degradation-rate of the modules can be assumed to be linear for a 25-year period, with an annual degradation rate of 0.25 percentage points per year. It is considered in the model by calculating the average yearly output ($\bar{P}_{PV}$) due to degradation over the lifetime of the plant (see Equation 3.18).

$$\bar{P}_{\mathrm{PV}} = P_{\mathrm{PV}} \cdot \frac{2 - \delta(t-1)}{2} \qquad \textit{Equation 3.18}$$

Where δ is the degradation rate and t is the lifetime (years).

3.4 Reverse Osmosis Plant

In both systems (system 1 and 2), the RO plant has been considered to have a SEC of 4 kWh/m^3 of produced water. The water production is calculated by Equation 3.19.

$$V_{\mathrm{water}} = \int \frac{P_{\mathrm{RO}}}{SEC}\, dt \qquad \textit{Equation 3.19}$$

Where V_{water} is the produces water (m^3) and P_{RO} is the power consumed by the RO plant (kW).

3.4.1. Controls

System 1 has been set to always operate at nominal power, with an availability of 95 %. The remaining 5 % are assumed to occur when there is no power generation from the CSP + PV plant. It has been assumed that all the generated power from power plant goes to the RO plant and any excess power (when $P_{\mathrm{CSP+PV}} > P_{\mathrm{goal}}$) is fed to the grid (case a) or dumped (case b). In the case of deficit in power production ($P_{\mathrm{CSP+PV}} < P_{\mathrm{goal}}$), then the grid will supply the extra power needed to reach P_{goal}.

In case of system 2, the production of water is not affected by any downtime due to maintenance since this is assumed to occur when there is no power production from the CSP + PV plant. Here it is considered that there is no grid available and that all excess power, which takes place when the power production is above P_{goal} or between two operation modes, is dumped. The flow chart of the control loops for a system 2 is presented Figure 3.3. It explains how pumps are turned on or off one by one to gradually change the water production and match the power generated by the CSP + PV plant.

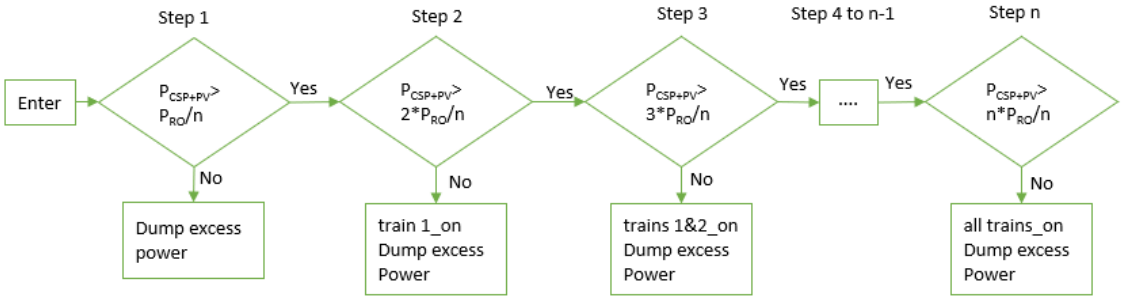

Figure 3.3: Flow chart of control loops for system 2. In this figure, P_{RO} is the rated power of the RO plant and n is the number of trains.

3.5 Technical Evaluation

This section presents the calculations used the technical evaluation.

3.5.1. CSP + PV Plant

The technical performance of the CSP + PV system was evaluated with regards to the CF of the system. CF can be evaluated by considering the total energy generated (case a) or by only considering the energy that is sent to the RO (case b). CF is defined by Equation 3.20.

$$CF_{\text{CSP+PV}} = \frac{E_{\text{tot}}}{P_{\text{goal}} \cdot 8760} \qquad \textit{Equation 3.20}$$

Where E_{tot} is the total annual electricity generation (kWh/year). This is, E_{tot_a} for "case a" and E_{tot_b} for "case b" and was calculated by Equation 3.21, considering a power limit of 15 MW for E_{tot_b}.

$$E_{\text{tot}} = \int (P_{\text{CSP}} + P_{\text{PV}})dt \qquad \textit{Equation 3.21}$$

3.5.2. RO Plant

The technical performance of system 1 was evaluated considering the solar fraction (*f*) of the electricity used. This is defined as the part of the total electricity used in the RO plant that comes from the CSP and PV plants. This was calculated by Equation 3.22. System 2 was evaluated regarding the CF of the RO plant using Equation 3.23. CF have not been considered for system 1 since it was assumed to always be at 95 % and solar fraction have not been considered for system 2, since it will always be at 100 %.

$$f = \frac{E_{\text{RO}}}{P_{\text{goal}} \cdot 8760 \cdot 0.95} \qquad \textit{Equation 3.22}$$

$$CF_{\text{RO}} = \frac{E_{\text{RO}}}{P_{\text{goal}} \cdot 8760} \qquad \textit{Equation 3.23}$$

Where E_{RO} is the electrical energy used in the RO plant (kWh) and 0.95 is its availability.

3.6 Environmental Evaluation

The environmental impact of the desalinated water, in terms of global warming, has been evaluated by focusing on the electricity used for running the RO plant and the impact from the construction of the RO plant is not considered. It has been assumed that the environmental impact for the RO plant is the same no matter the number of trains it has. Therefore, the key factor and the main difference between the systems is the emission factor of the used electricity. This is expressed as grams of CO_2 equivalents per kWh ($gCO_{2\text{-eq}}$/kWh). The average emission factor for the grid electricity in Kuwait (EF_{Grid}) is 767 $gCO_{2\text{-eq}}$/kWh [19]. According to a study by Kommalapati et al. [20], the average emission factor for central receiver CSP systems (EF_{CSP}) is 85.67 $gCO_{2\text{-eq}}$/kWh, with a mean standard error of 26.16 $gCO_{2\text{-}q}$/kWh. In the case of monocrystalline PV systems (EF_{PV}), the average emission factor is 73.68 $gCO_{2\text{-eq}}$/kWh, with a mean standard error of 10.76 $gCO_{2\text{-eq}}$/kWh [20]. In this study, an emission factor of 86 $gCO_{2\text{-eq}}$/kWh has been considered for the CSP plant and 74 $gCO_{2\text{-eq}}$/kWh for the PV plant. The total GWP of the water has been calculated by Equation 3.24 and is measured in $gCO_{2\text{-eq}}/m^3$. Electricity supplied to the grid have been assumed to decrease the contribution of fossil powered electricity to the grid and is thus subtracted from the total emissions of the system. The

average electricity mix for Kuwait have been used when evaluating the emission factor both for buying and selling to the grid, due to the merit order of electricity being unknown for Kuwait.

$$GWP = \frac{E_{\text{CSP}} \cdot EF_{\text{CSP}} + E_{\text{PV}} \cdot EF_{\text{PV}} + (E_{\text{buy}} - E_{\text{sell}}) \cdot EF_{\text{Grid}}}{V_{\text{water}}} \quad \textit{Equation 3.24}$$

Where E_{buy} is the annual electricity bought from the grid (kWh) and E_{sell} is annual the electricity sold to the grid (kWh)

3.7 Economic Evaluation

For the economic evaluation, the lifetime of the whole system has been assumed to be 25 years and the discount rate (r) 4 %.

3.7.1. CSP + PV Plant

The cost for the SF was calculated for different solar multiples in *SAM* using the default values suggested by the software (see Table 3.5*)*. A linear relation between the cost and the SM was obtained from these values and used in the model to ease the simulation process (see Equation 3.25).

$$C_{\text{SF}} = 19.76 * SM + 12.38 \quad \textit{Equation 3.25}$$

Where C_{SF} is the investment cost for the SF in MUSD.

Table 3.5 Input values used in SAM for calculating SF cost.

Parameter	*Symbol*	*Value*	*Unit*
Site improvement cost		16	USD/m^2
Heliostat field cost		140	USD/m^2
Heliostat field cost fixed		0	USD
Tower cost fixed	$C_{\text{t}_{\text{fix}}}$	3	MUSD
Tower cost scaling exponent	e_t	0.0113	-
Receiver reference cost	$C_{\text{r}_{\text{ref}}}$	103	MUSD
Receiver reference area	$A_{\text{r}_{\text{ref}}}$	1571	m^2
Receiver cost scaling exponent	e_r	0.7	-

The tower cost scaling exponent is the relation between tower cost and tower height (h_t) and is used by *SAM* when calculating the total tower cost C_{t} (see Equation 3.26) [21].

$$C_{\text{t}} = C_{\text{t}_{\text{fix}}}^{e_{\text{t}} \cdot \left(h_{\text{t}} - \frac{h_{\text{r}} - h_{\text{h}}}{2}\right)} \quad \textit{Equation 3.26}$$

Where h_{r} is the receiver height and h_{h} is the heliostat height (m).

The receiver cost scaling exponent is the relation between receiver cost and receiver area and is used by *SAM* when calculating the total receiver cost C_{r} (see Equation 3.27) [21].

$$C_{\text{r}} = C_{\text{r}_{\text{ref}}} \cdot \left(\frac{A_{\text{r}}}{A_{\text{r}_{\text{ref}}}}\right)^{e_{\text{r}}} \quad \textit{Equation 3.27}$$

Where A_{r} is the receiver area (m^2).

The rest of the costs for the CSP plant and the costs for PV plant are presented in Table 3.6. Values for the CSP plant are based on the default values in the cost calculator in *SAM*. Values for the PV plant are based on a report by Fu et al. [22].

Table 3.6 Economic values.

Parameter	*Value*	*Unit*
CSP costs		
TES cost	22	USD/kWh thermal
Balance of plant cost	290	USD/kW
PB cost	1040	USD/kW
Contingency cost	7	%
EPC and owner cost	13	%
Fixed O&M cost	66	USD/(kW year)
Variable O&M cost by generation	3.5	USD/MWh
PV costs		
Investment cost	1.06	USD/W
O&M cost	13	USD/(kW year)

LCOE are calculated by Equation 3.28 based on the simple LCOE calculator suggested by the National Renewable Energy Laboratory [23].

$$LCOE = \frac{crf \cdot (C_{\text{CSP+PV}}) + O\&M_{\text{CSP+PV}}}{E_{\text{tot}}} \qquad \textit{Equation 3.28}$$

Where $C_{\text{CSP+PV}}$ is the total cost for CSP and PV plant (USD), $O\&M_{\text{CSP+PV}}$ is the total operation and maintenance (O&M) cost for the CSP and PV plant (USD/year) and crf is the capital recovery factor, calculated by Equation 3.29.

$$crf = \frac{r(r+1)^t}{(r+1)^t - 1} \qquad \textit{Equation 3.29}$$

Where r is the discount rate and t is the lifetime (years).

3.7.2. RO Plant

The economic values for the RO plant were obtained from the cost estimator tool at desaldata.com [24], which is based on data from real RO plants. The input values used in the cost estimator are presented in Table 3.7. System 2, which uses multiple trains, is considered as multiple systems for the calculation of the investment costs. This means that the cost is estimated for one train and then multiplied by the number of trains to have the total investment cost. These costs are presented in Table 3.8.

Table 3.7: Input values used in the cost estimator.

Capacity Train n	90000/n m^3/day
Seawater Salinity	45000 mg/l
Seawater Min Temp	15 °C
Seawater Max Temp	32 °C
Pre-treatment	Difficult
Second Pass	0 %
Remineralization	Yes
Intake/Outfall	Typical
Permitting	Typical
Country	Kuwait

Table 3.8 Economic figures for the RO system depending on the number of trains [24].

Parameter	*Value*	*Unit*	*Increase (%)*
C_{RO1}	116	MUSD	0
$O\&M_{RO1}$	6.6	MUSD/year	0
C_{RO2}	129	MUSD	11.2
C_{RO3}	136	MUSD	17.2
C_{RO4}	141	MUSD	21.6
C_{RO5}	145	MUSD	25
C_{RO6}	148	MUSD	27.6
C_{RO7}	151	MUSD	30.2
C_{RO8}	154	MUSD	32.8

The cost for O&M has been assumed to increase with the number of trains in the same rate as the investment cost. Calculated O&M costs for a RO system with multiple trains are presented in Table 3.9.

Table 3.9 Calculated operation and maintenance costs for the RO system depending on the number of trains.

Parameter	*Value (MUSD)*
$O\&M_{RO2}$	7.34
$O\&M_{RO3}$	7.74
$O\&M_{RO4}$	8.02
$O\&M_{RO5}$	8.25
$O\&M_{RO6}$	8.42
$O\&M_{RO7}$	8.59
$O\&M_{RO8}$	8.76

The levelized cost of water (LCOW) was evaluated using Equation 3.30. Here the total cost for the whole system, CSP + PV + RO (C_{tot}), is considered. Also, the costs and gains from buying and selling electricity to and from the grid. The buy price was set to 0.05 USD/kWh [25] in the reference case and the sell price was set to 0. These are varied in the parametric study to see how the electricity market may favour different system designs. The cost for emission permits (or emission penalties), expressed in USD per tonne CO_2 equivalents ($USD/tCO_{2\text{-eq}}$), has also been added to see how this affects the price of the water and how it may push for a "cleaner" water production. Since this value is unknown for Kuwait, it is varied between 0 and 30 $USD/tCO_{2\text{-eq}}$ in this study based on the "cap and trade" price in European Union, which is around 28 $EUR/tCO_{2\text{-eq}}$ [26].

$$LCOW = \frac{crf \cdot (C_{\text{tot}}) + O\&M_{\text{tot}} + C_{\text{el}_{\text{buy}}} \cdot E_{\text{buy}} - C_{\text{el}_{\text{sell}}} \cdot E_{\text{sell}}}{V_{\text{water}}} + \frac{C_{\text{CAP}} \cdot GWP}{1\,000\,000} \qquad \textit{Equation 3.30}$$

Where $C_{\text{el}_{\text{buy}}}$ and $C_{\text{el}_{\text{sell}}}$ are the average electricity buy and sell prices (USD/kWh), C_{CAP} is the cost for carbon emission permits ($USD/tCO_{2\text{-eq}}$) and GWP the carbon emissions associated to the produced water ($gCO_{2\text{-eq}}/kWh$). 1 000 000 is to convert between gram and tonne.

4 Parametric Study

A parametric study was performed to analyse how TES size, SM and PV system size would affect LCOE, LCOW, CF, solar fraction, and GWP. This was done to find out which system design would give the lowest LCOW and GWP. The TES size was varied in 2 h steps between 2 h and 20 h and the PV size was varied in 4 MW steps between 0 MW and 32 MW. This was done for SMs of 2, 2.5, 3 and 3.5. Simulations were done for a whole year with 8760 h. For every simulation it was made sure that the initial state of charge of the TES was the same as in the end of the simulation.

4.1 CSP

Firstly, an analysis was carried out to find which combination of SM and TES size, in the CSP plant, would give the lowest LCOE and the result was used as a reference for the CSP + PV plant. This was followed by a sensitivity analysis of the TES price, where the cost of the TES was varied between 22 USD/kWh thermal (default input in *SAM*) and 45 USD/kWh thermal (as suggested by [27]).

4.2 CSP + PV

The parametric study of the CSP + PV plant has been divided into: technical evaluation, economic evaluation and sensitivity analysis. It has been evaluated technically regarding CF and economically regarding LCOE by varying the TES and PV size for different SMs as explained at the beginning of section 4. Since CF and LCOE may favour different CSP + PV designs, a total score is given by dividing LCOE by CF. This gives the cost for the CF in USD/(kWh %), and is a way to evaluate the gains for having a system storage compared to a system without storage.

A sensitivity analysis was done for the cost inputs with an uncertainty of ± 20 % for O&M and total investments costs.

4.3 System 1

The parametric study of system 1 has been divided into: technical evaluation, environmental evaluation, economic evaluation and sensitivity analysis. It was evaluated technically regarding CF, environmentally regarding GWP and economically regarding LCOW. In addition, the analysis of the affect that the grid electricity costs and emission penalties have on the LCOW of the produced water has been carried out.

As in section 4.2, a sensitivity analysis was done where the cost inputs for CSP and PV were varied by ± 20 %. Also, the GWP has been variated as follows: 86 ± 26 $gCO_{2\text{-}eq}$/kWh for the CSP plant and 74 ± 11 $gCO_{2\text{-}eq}$ for the PV plant.

4.4 System 2

Firstly, it has been analysed which combination of SM, TES size and PV size would give the lowest LCOW for a single train RO plant that varies its operation to match the available power at a constant SEC. The aim was to identify which CSP + PV design is the most suitable to be coupled with an off-grid RO plant. From these results three energy systems were selected: A PV plant, a CSP plant and a CSP + PV plant. These are used when investigating how the number of trains affect the CF and LCOE of system 2. The number of trains are varied between 1 train and 8 trains.

An uncertainty analysis was done regarding the cost increase of the RO plant due to the increase of the number of trains. A comparison was done between keeping the costs constant with the number of trains and the costs increase suggested in section 3.7.2. Also, an analysis was done where the cost inputs for the CSP plant and PV plant were varied by ± 20 %.

5 Results

This section presents the main results from the tests conducted in the study. All simulated and calculated results that are not shown in this section are presented in Appendix A and Appendix B.

5.1 CSP

Initially, an optimization of a CSP system is presented to see which combination of TES size and SM would give the lowest LCOE. This is followed by a sensitivity analysis of the TES price, with the aim to reveal if the optimal design would be different with a higher storage price (45 USD/kWh thermal instead of 22 USD/kWh thermal). The results presented in Figure 5.1 indicate that the optimal design of a CSP system (without PV) would be a SM of 3.5 and 14 h of storage.

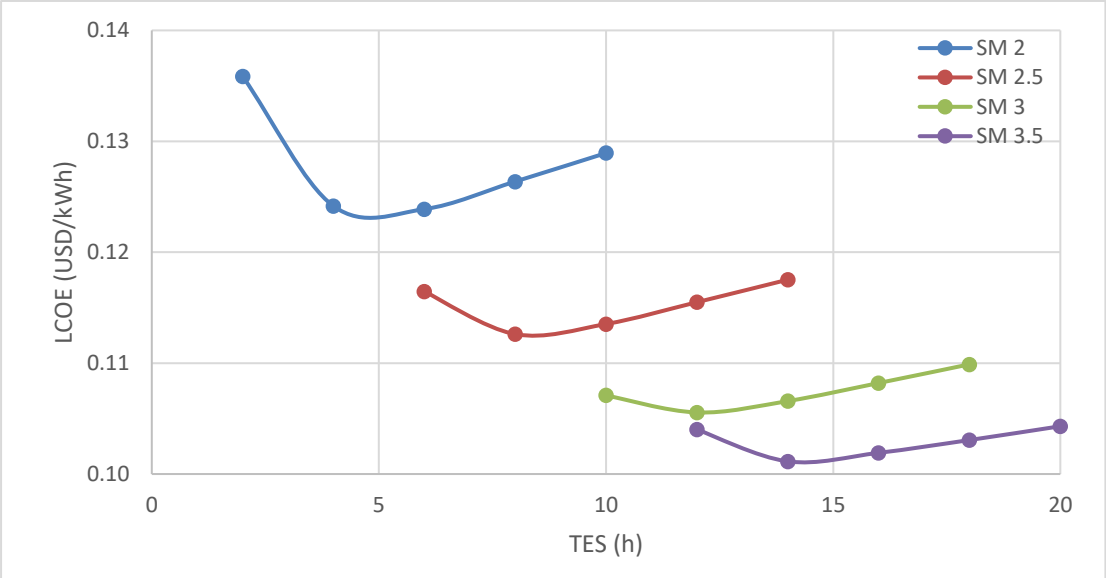

Figure 5.1 The relation between the LCOE and the TES size for four different SMs with a TES cost of 22 USD/kWh.

The optimal design would not change if the TES price is increased to 45 USD/kWh thermal according to Figure 5.2, though it will lead to an increase of the LCOE, from 0.101 USD/kWh to 0.112 USD/kWh for the optimal configuration.

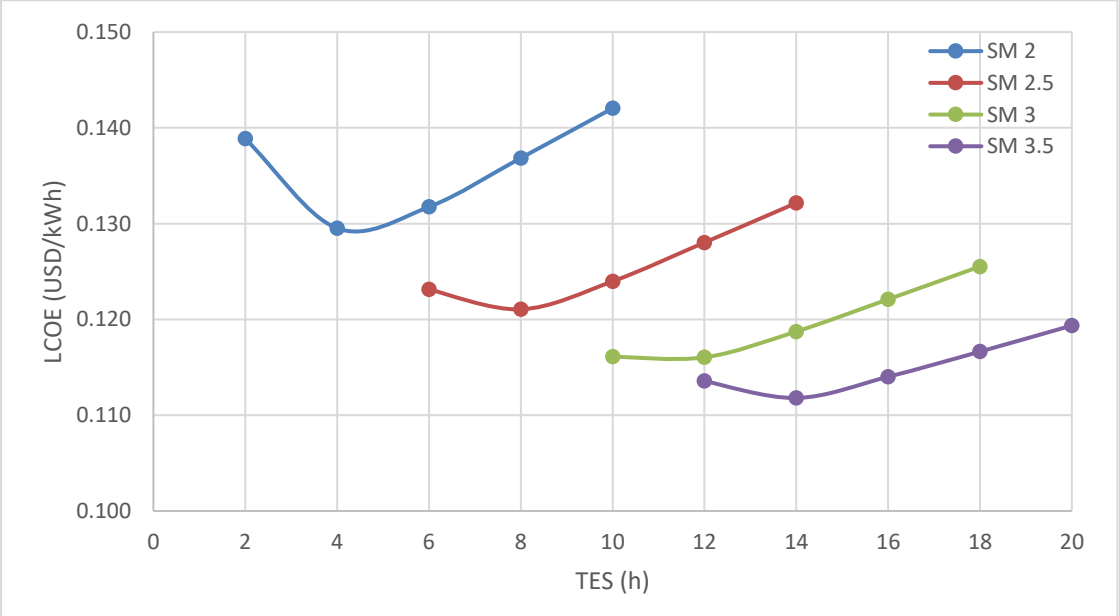

Figure 5.2 The relation between the LCOE and the TES size for four different SMs with a TES cost of 45 USD/kWh.

5.2 CSP + PV

As mentioned in Section 2, two cases are compared for system 1, since it is unknown if there are limits regarding how much power can be supplied to the grid: "Case a", where all excess power can be sent to the grid and "case b", where all excess power has to be discarded.

Four CSP designs (see Table 5.1) were used when analysing the impact that the PV plant has on CF, LCOE, LCOW, solar fraction and GWP. These designs are based on the results presented in Table B.3 and they are those that give the lowest LCOE, in "case b", for the four different SMs when adding PV to the system.

Table 5.1 The four CSP designs used in the study.

System	*SM*	*TES (h)*
CSP 1	2	12
CSP 2	2.5	14
CSP 3	3	14
CSP 4	3.5	14

5.2.1. Technical Evaluation

The technical performance of the CSP+PV system is evaluated regarding CF. Only "case b" is considered when analysing CF for the energy system, since it is defined for a 15 MW system according to Equation 3.20. Though this definition would not be correct when analysing a system with only PV, it is anyway done so here due to the whole energy system being defined as a 15 MW system, disregarding the size of the PV plant. In Figure 5.3 it is clearly shown how CF increases with bigger TES, the higher the SM and the bigger PV plant.

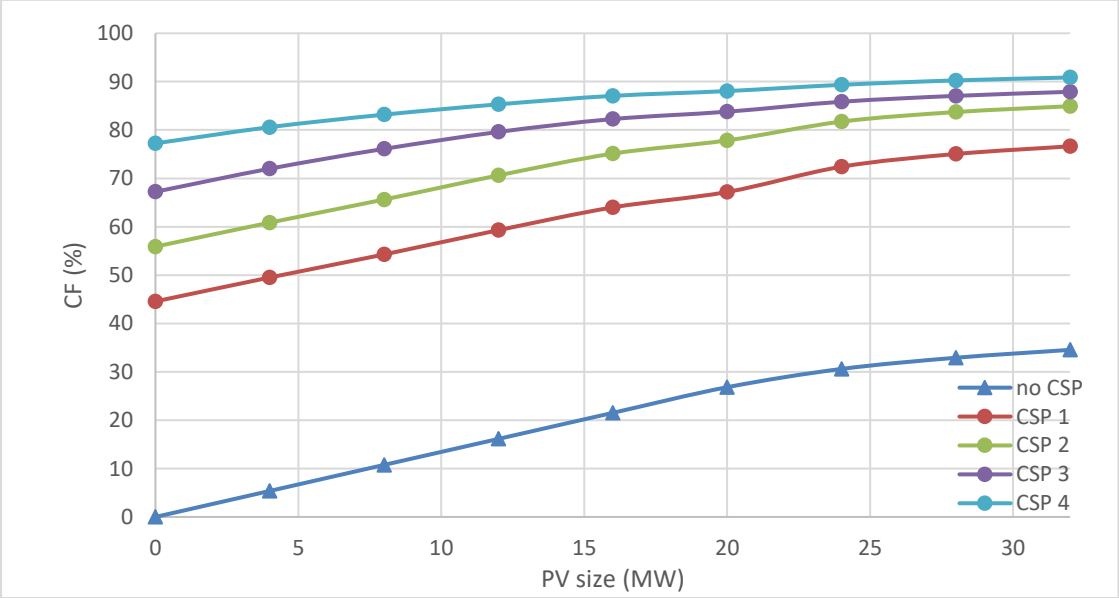

Figure 5.3 The relation between CF and PV size for different CSP designs for "case b".

For the system without CSP, the increase in CF starts to flatten out when the PV size exceeds 20 MW (blue line in Figure 5.3) due to the PV output exceeding 15 MW more frequently, which leads to more energy being discarded. For a system with CSP the increase in CF is almost linear until the PV size exceeds 16 MW where it flattens out. It goes up again at 24 MW before it starts flattening out (see red line in Figure 5.3). This is because, with 16 MW of PV the PV operates more frequently between 70 % and 100 % of 15 MW. This is when the CSP plant constantly operates at 30 % capacity which leads to a lower thermal efficiency in the PB and more energy being dumped because $P_{tot} > P_{goal}$. When the PV size is bigger than 20 MW, the power delivered by the PV plant is greater than 15 MW which leads to a shutdown of the PB, according to the control functions described in Figure 3.2. This reduces

the time when the PB runs at 30 % and reduces the amount of energy being discarded while saving thermal energy to be used when there is no solar irradiance available. The CF evens out again as the PV size exceeds 24 MW because of the high amount of power being dumped due to the oversize of the PV plant. This can be seen Figure 5.4 which shows the fraction of the total generated energy that is being discarded due to the total electrical power exceeding 15 MW.

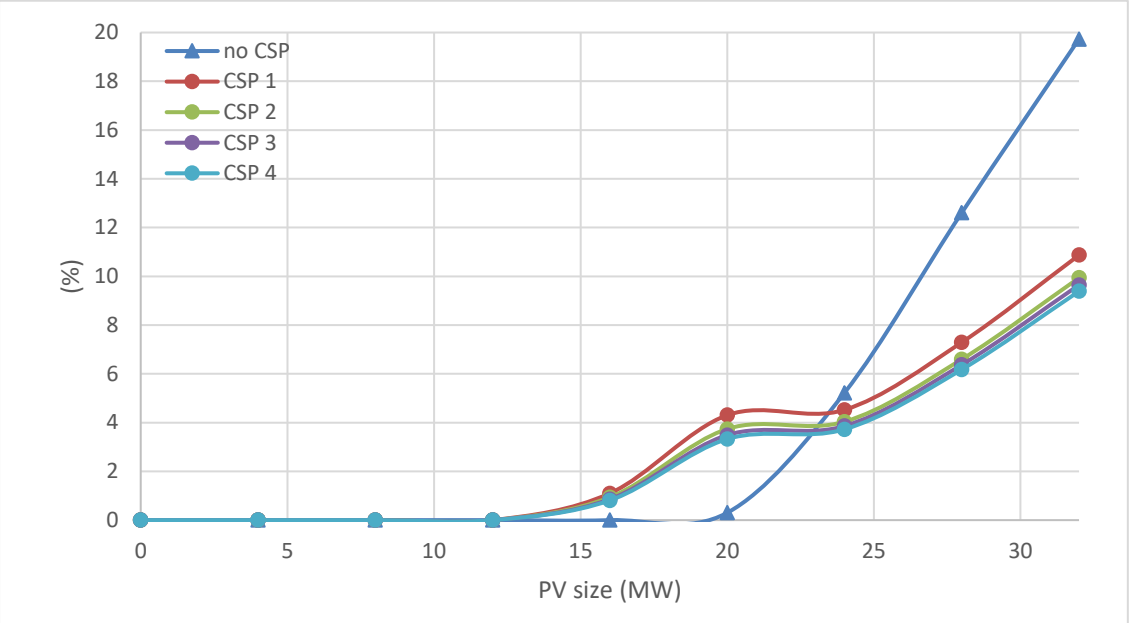

Figure 5.4 Fraction of total generated energy that is being discarded due to the generated power exceeding 15 MW for different energy systems.

All the results regarding the CF for the CSP + PV system are found in Table B.1. The highest CF is 0.92 and it is obtained with 20 h TES, SM of 3.5 and 32 MW PV. A CF of 0.35 can be reached with 32 MW PV.

5.2.2. Economic Evaluation

The economic performance of the CSP + PV system is analysed firstly by evaluating the LCOE of the system. Figure 5.5 presents a comparison of the LCOE for different CSP + PV combinations for "case a" and "case b". These graphs reveal an obvious difference in which combination of CSP and PV is optimal regarding LCOE for "case a" and "case b". For both cases, a PV-only system clearly has the lowest LCOE, with the deferens being an increase of LCOE as the PV size exceeds 20 MW for "case b". However, for the CSP + PV system, the LCOE falls with the PV size for "case a". The design with the lowest LCOE for "case a" is CSP 2 with a PV size of 32 MW. For "case b" the LCOE has an optimal point for all CSP designs within the tested range. The optimal CSP + PV design for "case b" would be CSP 2 with a PV size of 24 MW which gives a LCOE of 0.098 USD/kWh. This is a 2.8 % reduction compared to a CSP plant with 14 h TES and a SM of 3.5.

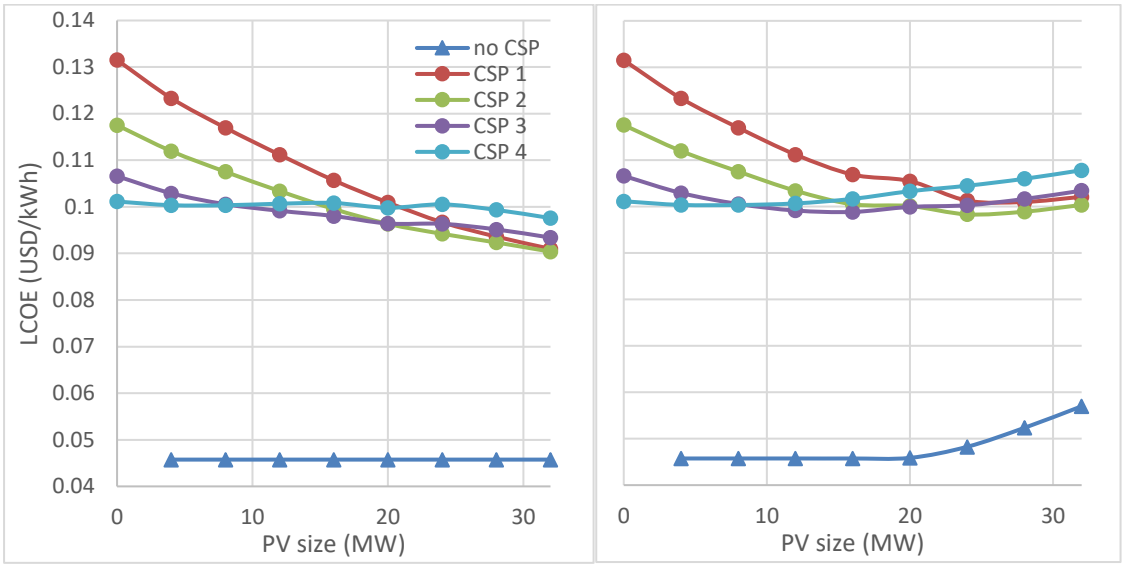

Figure 5.5 The relation between the LCOE and the PV size for different CSP designs for "case a" (left) and "case b" (right).

All the results regarding the LCOE are found in Table B.2 (case a) and Table B.3 (case b). For "case a" the lowest LCOE for a CSP + PV system is 0.09 USD/kWh and it is obtained with 14 h TES, SM of 2.5 and a PV size of 32 MW.

The LCOE for a PV-only system is, as mentioned, far lower than for a CSP + PV system. However, it does not consider that the storage in the CSP plant provides a higher CF and the ability to generate power when there is no solar irradiance available. The fraction of LCOE per CF for "case b" is shown Figure 5.6, in order to evaluate the cost due to the increase of the CF of the system. This gives an idea of which system is the most suitable to run a standalone RO plant. This analysis shows that it is favourable to have a CSP plant in the energy system. The most optimal design regarding LCOE per CF is CSP 3 with a PV size ranging between 24 – 28 MW, which results in values around 0.00117 USD/(kWh %).

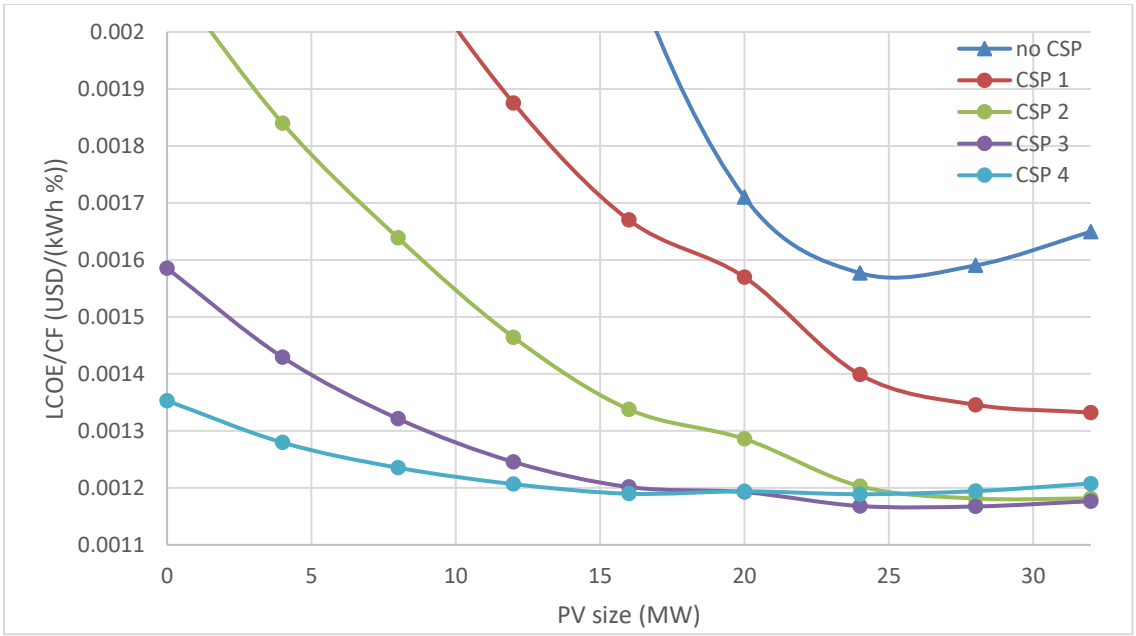

Figure 5.6 LCOE divided by CF for different PV sizes and CSP designs for "case b".

5.2.3. Sensitivity Analysis

Considering an uncertainty of ± 20 % for the costs of the CSP and PV plants, a PV-only system will still have a lower LCOE than a system with CSP. Then the optimal design for CSP + PV (for case b) is in the range of 0.079 – 0.119 USD/kWh and PV is in the range of 0.037 – 0.055 USD/kWh. Though varying the price of CSP and PV will alter which design

of CSP + PV is optimal. This is shown Figure 5.7 where the effects of the CSP price variation by ± 20 % while the PV price is constant are presented.

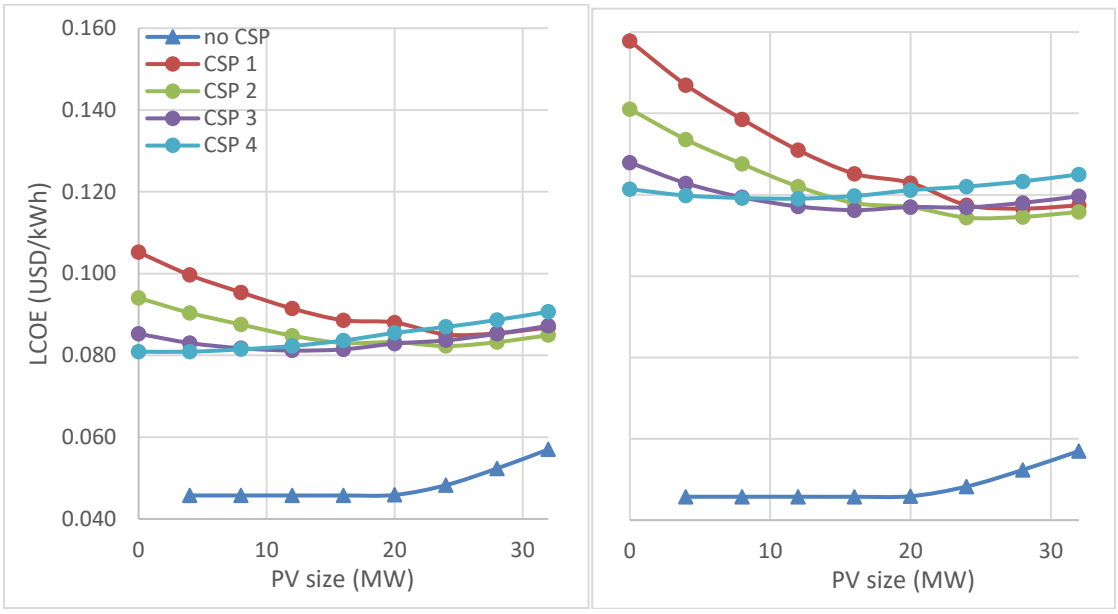

Figure 5.7 LCOE for different energy system designs with the CSP costs reduced by 20 % (left) and increased by 20 % (right).

Evaluating the system regarding LCOE/CF could favour a PV-only system considering a 20 % uncertainty. This is shown in Figure 5.8 where the CSP costs are increased by 20 % and the PV costs are reduced by 20 %.

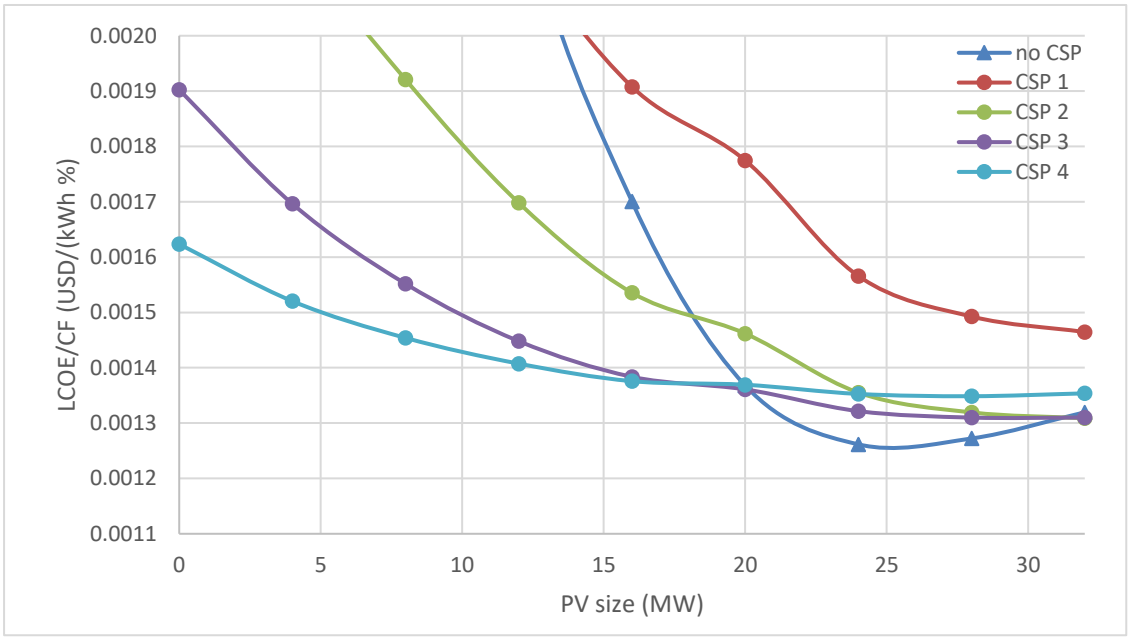

Figure 5.8 LCOE divided by CF for different energy system designs with the CSP costs reduced by 20 % and the PV costs increased by 20 %.

5.3 Parametric Study: System 1

This section presents the results from the parametric study of system 1.

5.3.1. Technical Evaluation

System 1 is technically evaluated with regard to the solar fraction of the electricity used in the RO plant. The results are presented in Figure 5.9, and they show a similar trend as the CF for the energy system in case b. It confirms that a system with CSP and TES gives a

significantly higher solar fraction that a system with only PV. The highest solar fraction (96 %) is reached for CSP 4 and a PV size of 32 MW.

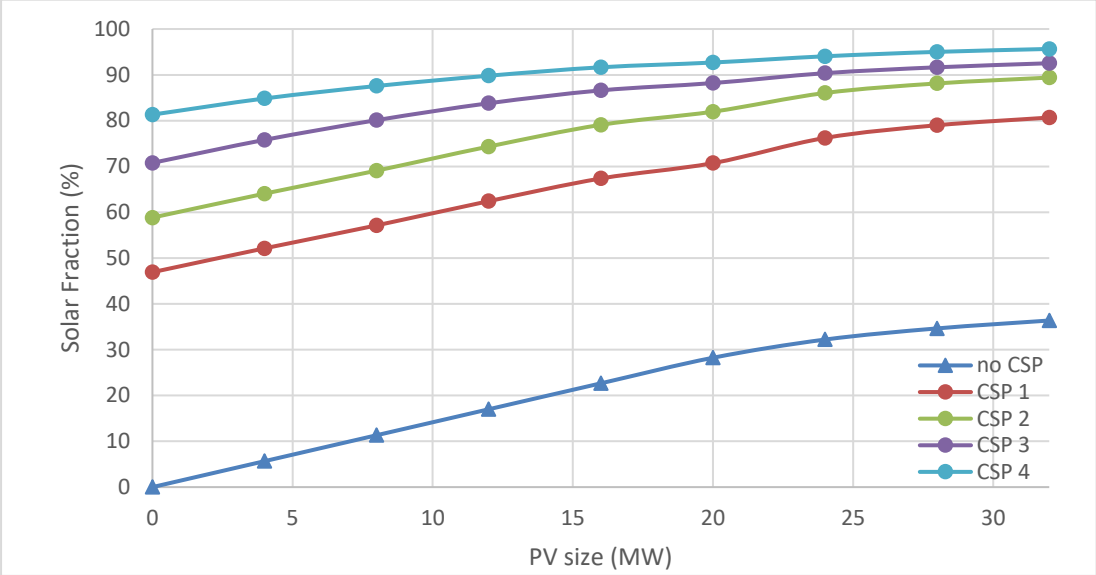

Figure 5.9 The solar fraction for system 1 depending on CSP design and PV size.

All the results regarding the solar fraction of system 1 can be found in Table B.4. The highest solar fraction is 0.97 and it is obtained with 20 h TES, SM of 3.5 and PV size of 32 MW. The highest solar fraction obtained for a PV plant is 0.36 for a PV size of 32 MW.

5.3.2. Environmental Evaluation

The GWP of the produced water for different CSP designs at variable PV size is presented in Figure 5.10, for "case a" and "case b". It shows how the GWP is greatly reduced the bigger the PV and the CSP plants are. The emission is further reduced in "case a" compared to "case b", since it has been assumed that 1 kWh of energy fed to the grid equals 1 kWh reduction of fossil powered electricity to the grid. The GWP of the produced water can then be lower than if the RO plant would have a 100 % solar fraction without selling electricity to the grid. Which would give a GWP in the range of 280 – 340 $gCO_{2\text{-eq}}/m^3$ for the produced water depending the mix of energy from CSP and PV. The lowest simulated values for "case a" and "case b" are 161 $gCO_{2\text{-eq}}/m^3$ and 465 $gCO_{2\text{-eq}}/m^3$, respectively.

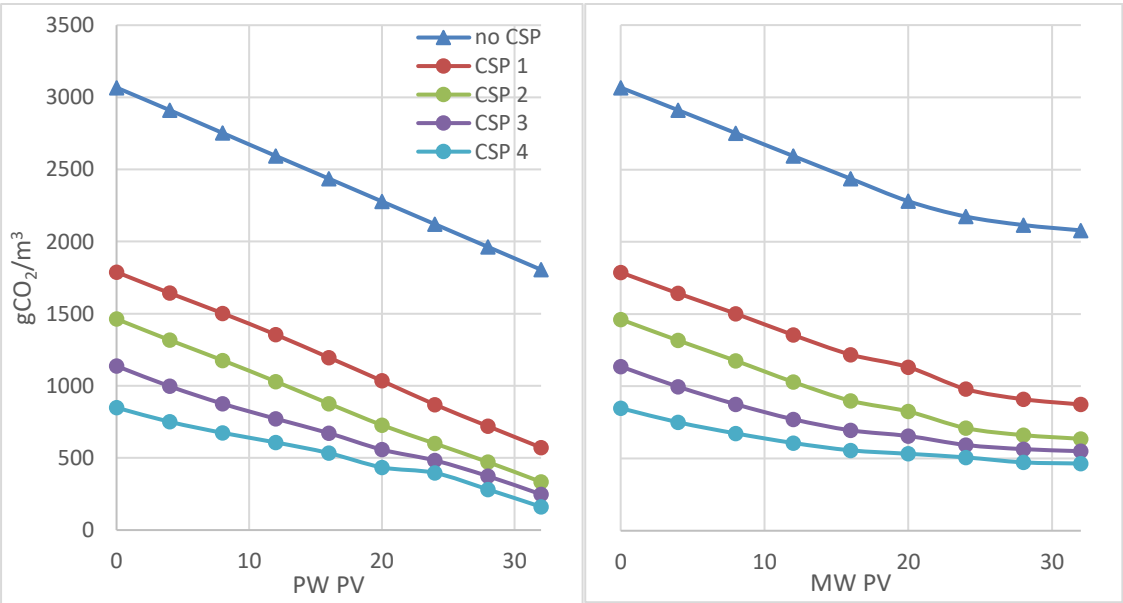

Figure 5.10 GWP for the produced water depending on CSP design and PV size, for "case a" (to the left) and "case b" (to the right).

All the results regarding GWP for system 1 can be found in Table B.5 (case a) and Table B.6 (case b). For "case a", the lowest GWP is 133 $gCO_{2\text{-eq}}/m^3$ and it was obtained with 20 h TES, SM of 3.5 and a PV size of 32 MW. For "case b", lowest value is 438 $gCO_{2\text{-eq}}/m^3$ and it was obtained with the same system as for case a.

5.3.3. Economic Evaluation

This section gives the results of the water costs and analyses how the price of electricity and emission permits may alter the choice of energy system. The reference case used considers a cost for buying electricity of 0.05 USD/kWh and does not consider any costs for emissions or revenue from selling electricity. Figure 5.11 shows the results of LCOW as a function of the PV size for different CSP designs for the reference case and a case where the electricity price is 0.10 USD/kWh for buying from the grid and 0.05 USD/kWh for selling to the grid.

In the reference case, it is shown that it is clearly better to have no CSP in the system due to the LCOE being much higher than the electricity price. The LCOE of the PV is a bit lower than the cost of the electricity from the grid which gives a small reduction to the LCOW compared to using only the grid. The lowest LCOW (0.645 USD/m^3) is obtained with a PV size of 20 MW. With more PV there is too much excess power that does not contribute to any reduction in costs. The optimal CSP + PV design (of those compared) is CSP 1 with a PV size of 12 MW, which results in a LCOW of 0.802 USD/m^3.

In the other case, it is more favourable to have CSP + PV than in the reference case, although it is still better to have only PV. The effects of selling electricity can be visible when the PV size exceeds 20 MW. There the LCOW of CSP system 3 and 4 flattens out instead of increases. The CSP + PV design that has the lowest LCOW in this case is CSP 2 with a PV size of 32 MW which results in a LCOW of 0.831 USD/m^3. The best PV design has the size of 32 MW, which results in a LCOW of 0.769 USD/m^3.

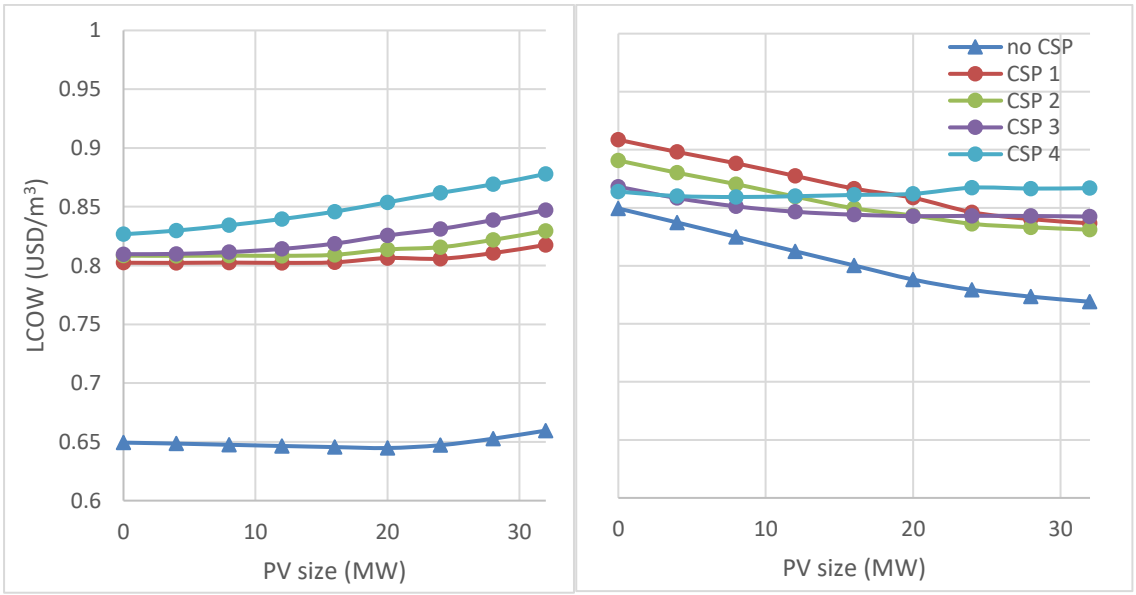

Figure 5.11 LCOW for system 1 for different PV sizes and CSP designs, with electricity prices of 0.05 USD/kWh for buying and 0.00 USD/kWh for selling (left) compared to 0.1 and 0.05 USD/kWh (right).

All the results of LCOW, considering the prices from the reference case, can be found in Table B.7.

The breakpoint that indicates when the electricity price favours a system with CSP, without considering the sell price, is revealed in Figure 5.12. Five different designs for the energy system, based on results presented in Figure 5.5, have been compared to only using the grid. The results show that a system with CSP + PV is more economically feasible than a PV-only

system when the electricity price is higher than 0.13 USD/kWh and better that only using the grid if the electricity price is higher than 0.1 USD/kWh.

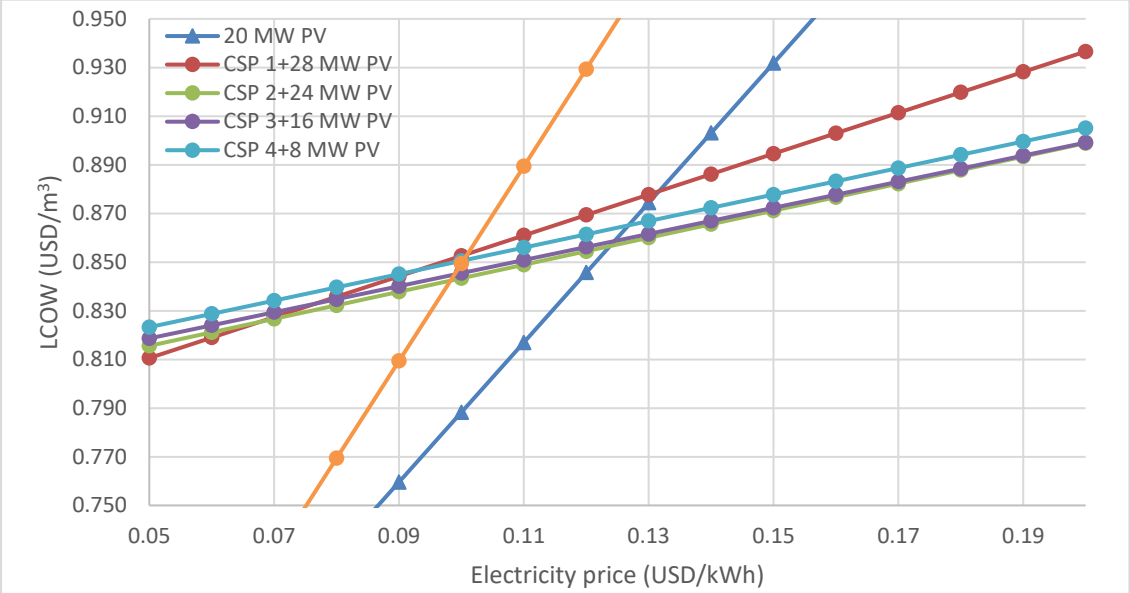

Figure 5.12 LCOW as a function of the price of bought electricity for different energy systems, considering case b.

In Figure 5.13 it is shown how the cost for buying emission permits (or emission penalties) affects the LCOW for different system designs. The aim is to find the price level that would make the use of a system with a high solar fraction more lucrative when the electricity price is 0.05 USD/kWh compared to 0.1 USD/kWh. The results show that, with an electricity price of 0.05 USD/kWh (which is the present case for Kuwait), the price of emission permits would have to be slightly higher than 70 USD/$tCO_{2\text{-eq}}$ to make a CSP + PV plant more economically feasible than using the grid. A PV-only system is however better that only using the grid even without any emission permits. With an electricity price of 0.1 USD/kWh some CSP + PV designs will give a lower LCOW than only using the grid without any emission cost. In this case, a CSP + PV system would be competitive compared to a PV-only system if the emission price is higher than 30 USD/$tCO_{2\text{-eq}}$.

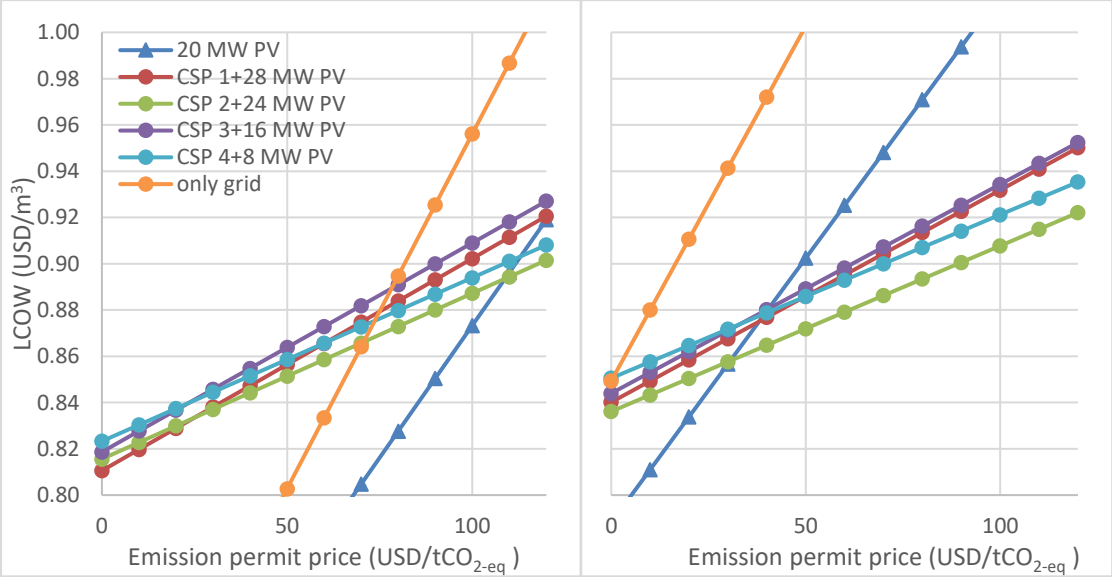

Figure 5.13 LCOW as a function of the price of emission permits for different energy systems, for case b, considering an electricity price of 0.05 USD/kWh (left) and 0.1 USD/kWh (right).

5.3.4. Comparison between LCOW and GWP

Figure 5.14 shows the change in LCOE and GWP when coupling RO with CSP and/or PV compared to the use of the grid. This was done for "case b" with the same cost inputs as in

the reference case from section 5.3.3. This reveals that a PV plant can reduce the GWP by 29 % without increasing the LCOW and 32 % with a cost increase of 1.6 %. With CSP + PV the GWP can be reduced by 85 % but with a 35 % increase in LCOW.

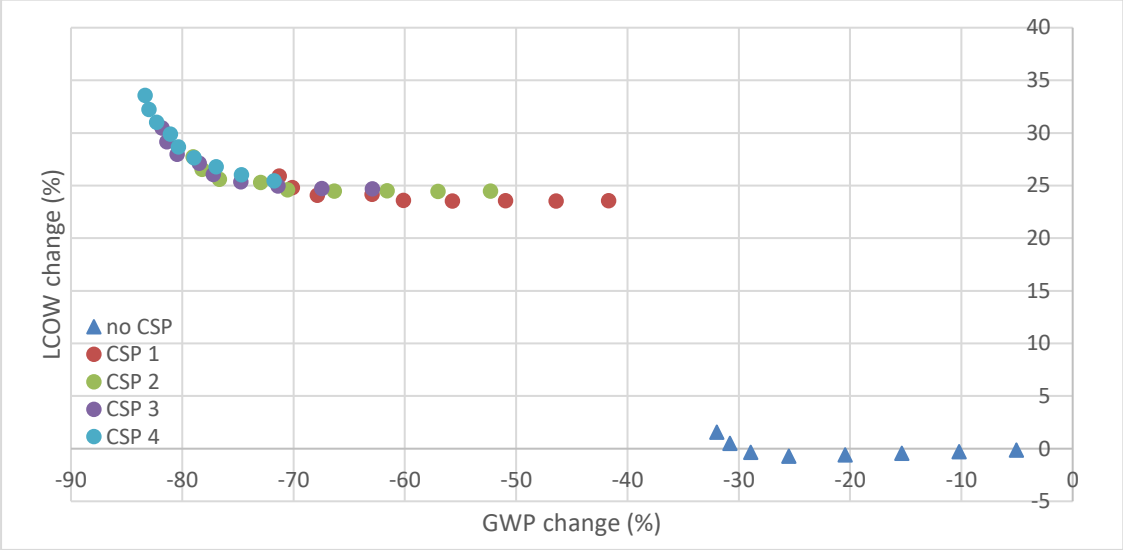

Figure 5.14 The relation between LCOE and GWP for the different energy systems at variable PV size, case a.

5.3.5. Sensitivity Analysis

The impact that the emission factors of PV and CSP have on the GWP is analysed by varying this factor by ± 11 $gCO_{2\text{-eq}}$/kWh for PV and ± 26 $gCO_{2\text{-eq}}$/kWh for CSP. The results are presented in Figure 5.15 where a reduction by 11 $gCO_{2\text{-eq}}$/kWh for the PV plant and increase by 26 $gCO_{2\text{-eq}}$/kWh for CSP plant is compared to an increase by 11 $gCO_{2\text{-eq}}$/kWh for PV plant and reduction by 26 $gCO_{2\text{-eq}}$/kWh for CSP plant. This analysis has been done for "case b". It shows that the emission factors of CSP and PV have just a notable impact on the GWP for the CSP + PV designs that have a high solar fraction, and that the lowest LCOW is obtained with CSP 4 plus a PV size of 32 MW.

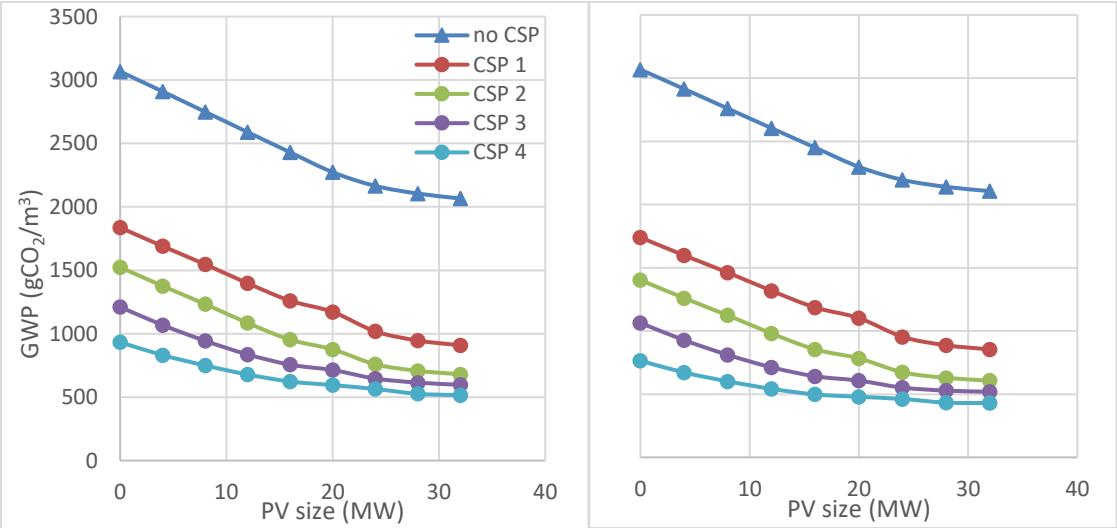

Figure 5.15 Comparison of how the emission factors of CSP and PV affect the GWP of the produced water. A decrease of 11 $gCO_{2\text{-eq}}$/kWh for the PV and increase of 26 $gCO_{2\text{-eq}}$/kWh for the CSP (left) compared to an increase of 11 $gCO_{2\text{-eq}}$/kWh for the PV and a decrease of 26 $gCO_{2\text{-eq}}$/kWh for the CSP (right).

In Figure 5.16 it is shown how the LCOW varies when the costs for CSP and PV are varied by ± 20 %. It compares a cost reduction for the CSP plant and a cost increase for the PV plant with respect to a cost increase for the CSP plant and a cost reduction for the PV plant. The electricity prices are the same as in the reference case. This shows that the cost of the

CSP and PV has a significant impact on the LCOW and can affect in the selection of the best CSP + PV design for this application.

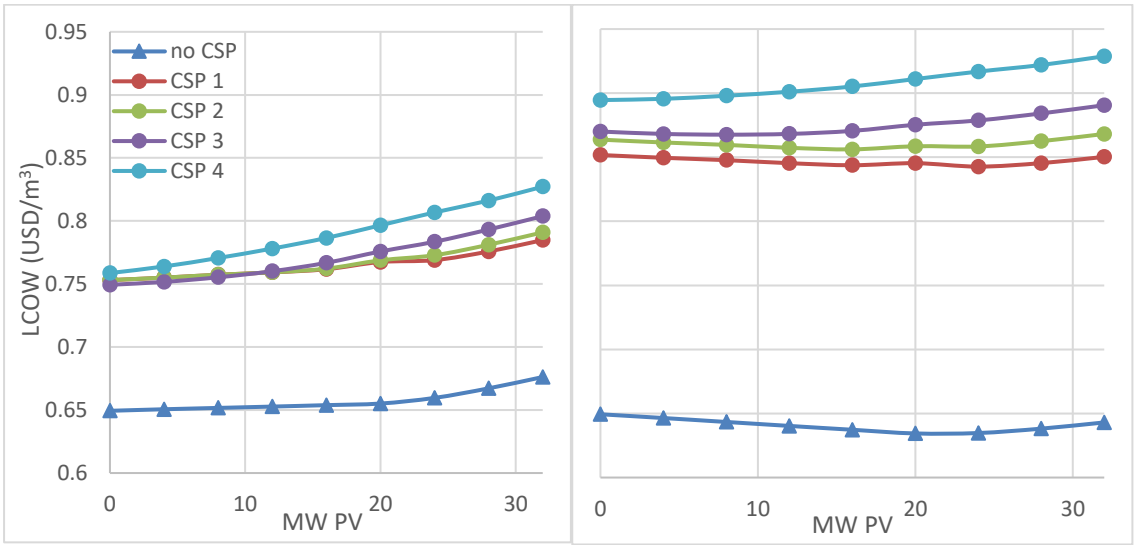

Figure 5.16 LCOW for different CSP + PV designs, with a 20 % cost reduction for the CSP plant and a 20 % increase for the PV plant (left) compared to a 20 % increase for the CSP plant and a 20 % reduction for the PV plant (right).

5.4 Parametric Study: System 2

Firstly, an analysis has been done for a single-train off-grid RO plant that can vary its operation at constant SEC, to match the available power. The aim was to get an indication to which energy system would be the most suitable for running an off-grid RO plant. The results obtained from this analysis are presented in Table B.8. From this analysis, three systems were selected for the parametric study of system 2 at variable number or trains. The three energy systems (a PV plant, a CSP plant and a CSP + PV plant) are presented in Table 5.2.

Table 5.2 PV, CSP and CSP + PV plant used in the parametric study of system 2.

Technology	*PV size (MW)*	*TES (h)*	*SM*	*LCOW (USD/m³)*
PV plant	32	-	-	1.46
CSP plant	-	16	3.5	0.96
CSP + PV plant	28	16	3	0.89

5.4.1. Technical Evaluation

System 2 is evaluated technically regarding the CF of the RO plant. The results obtained of the CF for the RO plant with a PV, a CSP + PV or a CSP plant at variable number of trains are presented in Figure 5.17. It was found that the RO plant with PV had the highest variation in CF when the number of trains varied, obtaining the highest increase (from 23.2 % to 30.4 %) when the number of trains was varied from one to three. This is because the PV plant has the most gradually variation in production, hence the most to gain from increasing the number of trains. The maximum capacity factor for the RO plant with PV (of 33 %) is obtained with 7 or 8 trains.

The highest CF (of 87.7 %) is obtained when the RO plant is driven by the CSP + PV plant and has four trains. In this case, the CF is increased by only 1 % when the number of trains is increased from 1 to 4.

For the case when the RO plant is driven by a CSP plant the CF is 77.2 % and there is no change in CF with the number of trains. This is because there is never any gradual change

in the power generation of the CSP plant, thereof nothing to gain from increasing the number of trains.

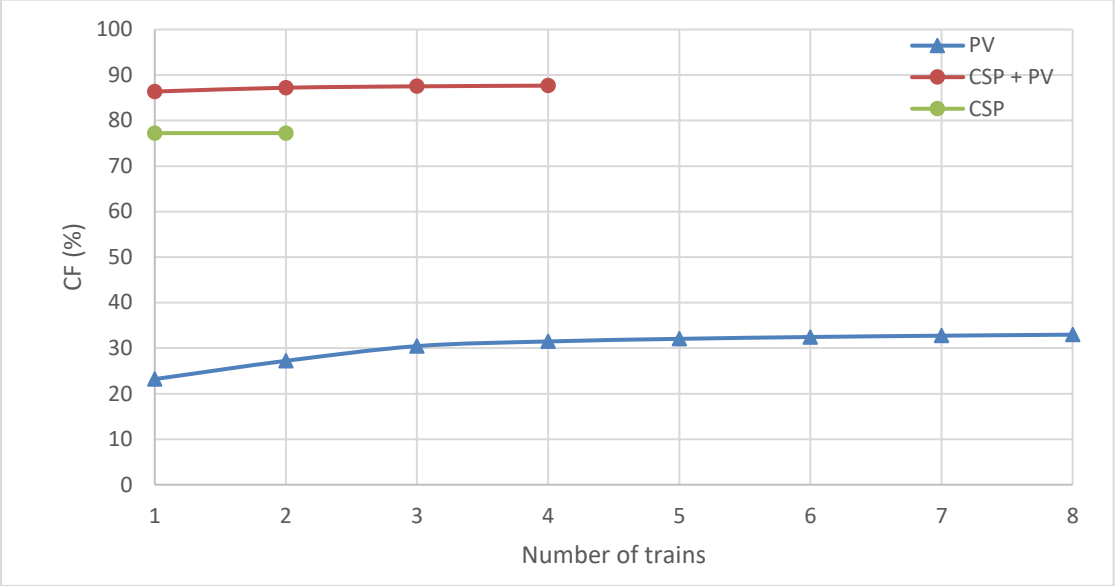

Figure 5.17 CF for system 2 as a function of the number of trains for three different energy systems.

This analysis has been complemented by the assessment of the self-consumption i.e. the fraction of generated electricity that is consumed by the RO plant. In the results presented in Figure 5.18, it is clear that there is no excess energy in the case of the CSP plant and that 53.9 % of the energy generated by the PV plant is consumed when the RO plant only has one train. In the case of the PV plant, a maximum self-consumption of 76.6 % was obtained and in the case of the CSP + PV plant, a maximum self-consumption of 93.1 %.

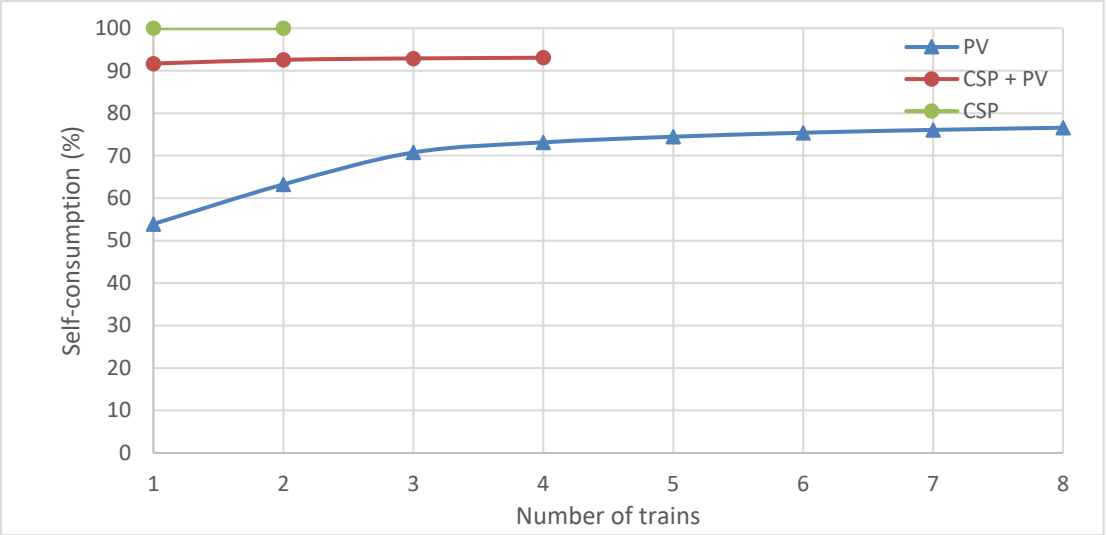

Figure 5.18 self-consumption of energy for system 2 as a function of the number of trains for the different energy systems.

5.4.2. Economic Evaluation

The change in the LCOW as a function of the number or trains is presented in Figure 5 19. This figure also shows a sensitivity analysis for the cost increase of the RO plant when the number of trains is increased, where the costs proposed in Table 3.8 and Table 3.9 are compared to keeping the costs constant with the number of trains.

According to the results shown, the RO plant with PV results in the highest LCOW for the produced water. When considering a cost increase for the RO, the lowest LCOW for the PV plant is 1.87 USD/m^3 and is obtained with four trains. Without cost increase the lowest LCOW is 1.50 USD/kWh and is obtained with eight trains. It was found that the LCOW is

reduced to 0.96 USD/m^3 when using the CSP plant and a single train, which is a reduction of 49 % compared to the PV plant (when considering a cost increase for the RO plant). The CSP + PV plant gave the lowest LCOW, 0.91 USD/m^3, with one train. It means a reduction of 5.3 % compared to the CSP plant.

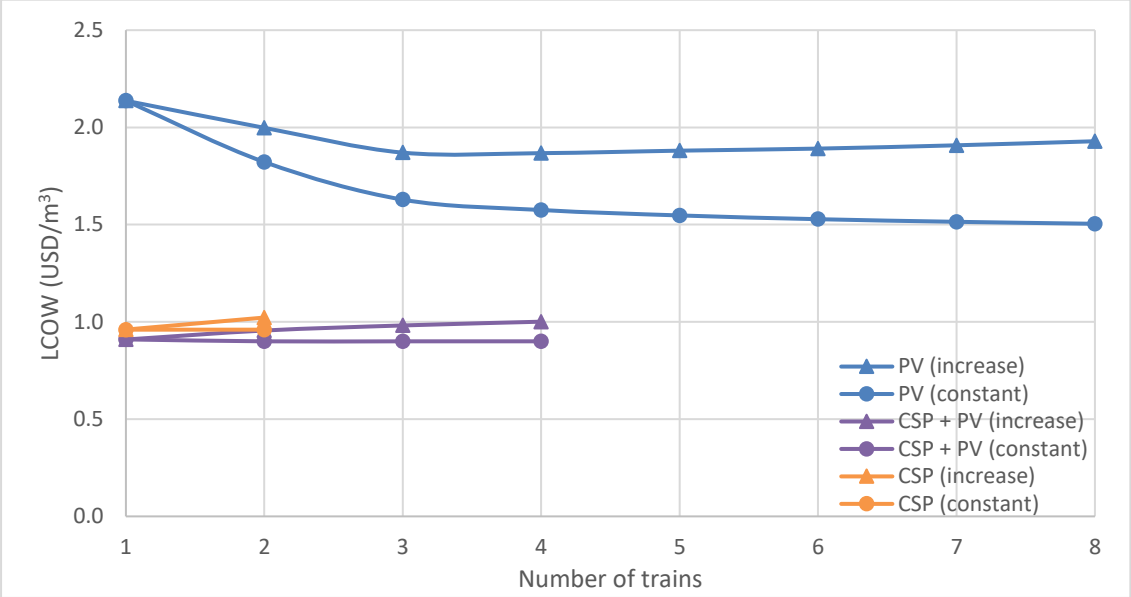

Figure 5 19: LCOW for system 2 in different configurations of trains and three different energy systems. Showing the cost range between having a cost increase for the RO plant with the number of trains and keeping the costs constant.

5.4.3. Sensitivity Analysis

Varying the costs for CSP and PV by ± 20 % varies the LCOW between 1.82 – 1.91 USD/m^3 for the PV + RO plant with four trains, 0.83 – 0.99 USD/m^3 for the CSP + PV + RO plant with one train and 0.88 – 1.04 USD/m^3 for the CSP + RO plant with one train. In Figure 5.20 it is shown that the CSP + PV plant always gives the lowest LCOW.

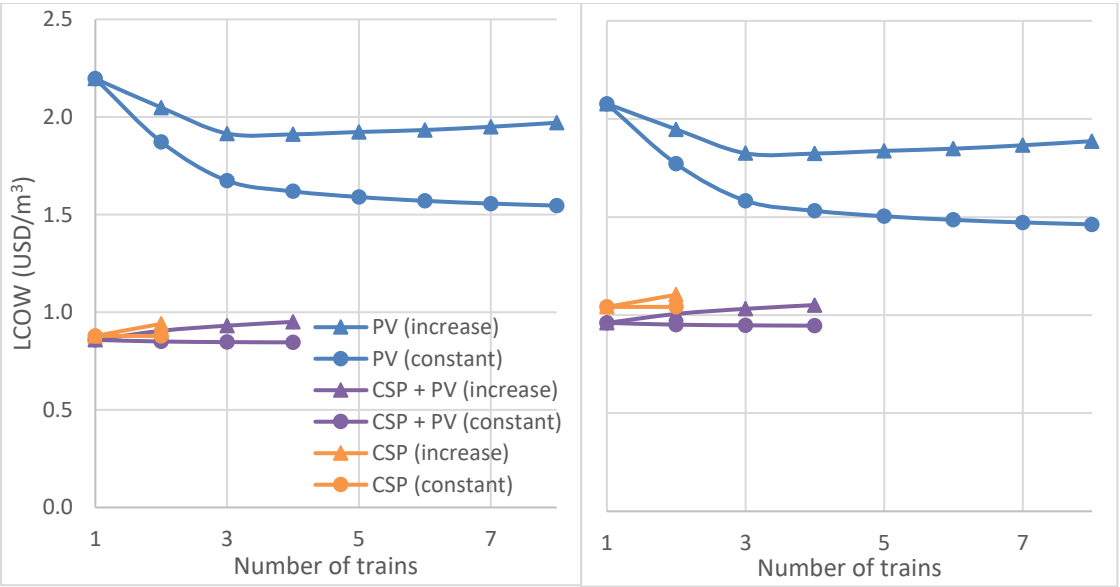

Figure 5.20 LCOW for system 2 in different configurations of trains and three different energy systems. Showing the cost range between having a cost increase for the RO plant with the number of trains and keeping the costs constant. Considering a 20 % cost reduction for the CSP plant and a 20 % increase for the PV plant (left) compared to a 20 % increase for the CSP plant and a 20 % reduction for the PV plant (right).

6 Discussion

This section discusses the results from this study as well as the simplification and assumptions made.

6.1 On-grid system

The results show that it is far cheaper to use PV to reduce the carbon emissions of an on-grid RO plant compared to CSP or CSP + PV. Though with the limitation that it cannot reduce GWP with much more than 32 % compared to only using the grid and has a maximum solar fraction of around 35 %. A CSP plant can reach a solar fraction higher than 80 % while reducing the GWP with more that 71 %. This comes with a 26 % increase in LCOW. With a CSP + PV plant the GWP can be reduced even further but at a higher cost.

These results are very dependent on the price of electricity as shown in Figure 5.12. With electricity cost above 0.10 USD/kWh, powering a RO plant with a CSP + PV plant would be competitive to only using the grid and with a cost above 0.13 USD/kWh it would be competitive to a PV-only plant. With the considered electricity price for Kuwait (0.05 USD/kWh) it would take an emission allowance cost (emission penalty) of more than 70 USD/$tCO_{2\text{-eq}}$ for a CSP + PV plant to compete with the grid which is more than 40 USD/$tCO_{2\text{-q}}$ higher than the "cap and trade" price in the European Union.

As mentioned in the introduction, it is important to have a low GWP for the desalinated water as the demand for it will increase in the future. The question is then if it is better to decrease the GWP by 30 % for many desalination plants by coupling them with PV without increasing the LCOW or by coupling a few RO plants with CSP + PV with a solar fraction above 90 % but a significant increase in LCOW. This would depend on (among other things) the ambition in the country regarding a fossil free water production and on the stability of the grid. A PV only system would bring more fluctuations in the power grid and could affect other sectors that are dependent on the grid while a CSP or CSP + PV system could supply power to the RO plant without disturbing the balance in the grid. If the goal would be that all new desalination plants should be more or less fossil free, then this could be achieved with CSP + PV + RO.

6.2 Off-grid system

In case of the off-grid system, it is clearly not feasible use a PV plant without storage for powering a RO plant. The RO plant stands for the biggest portion of the total investment costs and even though the PV plant generate power at low cost it does not make up for the low water production due a to low capacity factor. Also, the RO plant must be more complex to be able to follow the varying power generation from the PV plant. A CSP plant gets a much lower LCOW and higher CF than a PV plant. By combining CSP and PV, the LCOW can be reduced by 5 % and CF can be increased by 12 % compared to only CSP.

The results regarding the off-grid RO plant can be compared to the results from the study by Laissouis et al. [8], where an off-grid RO plant with CSP or PV was analysed. In his study, the best CSP + RO plant obtained an LCOW of 0.85 USD/m^3 whereas in this study the CSP + RO plant had a LCOW of 0.96 USD/m^3. The difference can be explained by differences in system design and boundary conditions like solar irradiation, SEC, etc. This demonstrates that the results obtained from this study are reasonable.

6.3 Sources of error

There are many assumptions and simplifications in the model and in the calculations. The main ones are as follows:

- Economic values: The cost inputs for the economic calculations have a significant impact on the LCOE and the LCOW as shown in the sensitivity analysis. Other values that are not analysed in the sensitivity analysis and could affect the result would be: the cost of the RO plant, discount rates and lifetime of the system.

- RO plant model: No real model of the RO plant was used in the simulations. Only the specific energy consumption was considered, which was assumed to be constant. This was due to time limitation. A detailed, dynamic model of the RO plant could give a more realistic operation of the RO plant, which would probably give a small difference in LCOW.

- Power block model: The PB performance is only expressed with two equations, to give the thermal efficiency depending on the ambient temperature and other related to the variability depending on the load fraction. A dynamic model considering all components would make the simulations more realistic. Though this was not possible within the timeline of the project. The efficiencies obtained are though reasonable, so the results are likely not too far from reality.

- Inertia in the CSP plant: The model of the CSP does not consider any inertia in the system, assuming that the PB can react instantly to changes in the demand and that it can turn on and off without any delay. For the on-grid case, a slower reaction time in the CSP plant would affect how much energy is bought from or sold to the grid. For the off-grid case, this would affect the design of the RO plant regarding the number of trains, due to more gradual variations in the CSP plant power generation.

- The emission factor of the grid is assumed to be the same along the whole year. This is not strictly true because it would vary depending on the demand and energy mix at the specific moment in time. This could affect which system would contribute to the highest reduction in carbon emissions since PV only operates during the day while CSP is dispatchable.

- The electricity price is also assumed to be constant over time but in a real scenario, it could vary depending on the electricity market.

7 Conclusions

The main conclusions are as follows:

- There is a great difference between the on-grid and the off-grid case regarding which energy system gives the lowest cost of the produced water.

- What solution is best suited for powering an on-grid RO plant strongly depends on how environment and economy are prioritised. The emissions can be reduced by ca 30 % with a PV plant, compared to only using the grid, while barely increasing the cost of the water. With a CSP + PV plant, the emission can be reduced by 85 % but with a cost increase of 35 % for the water.

- The price of electricity has a strong impact on which energy system is best suited for powering an on-grid RO plant.

- It is possible to motivate more renewable energy in the system by adding a cost for carbon emissions allowances. The emission cost required depends a lot on the electricity price. Adding an emission allowance cost of 70 USD/$tCO_{2\text{-}q}$ would make a CSP + PV plant competitive to the grid if the electricity price is 0.05 USD/kWh.

- It is not reasonable to power an off-grid RO plant with only PV due to the low capacity factor and high cost of water.

- It is possible to have an off-grid RO plant that is 100 % powered by CSP + PV. The cost of the water would then be around 0.9 USD/m^3.

- Coupling an off-grid RO plant with CSP + PV can bring a 5 % reduction in water cost and 12 % increase in water production compared to having only CSP.

8 Future Work

As mentioned in the discussion, there are many simplifications in the model of the CSP and the RO plants. Developing a more sophisticated model of the complete system where most components in the RO plant and the CSP plant are considered would reduce uncertainty in the results and would allow a more detailed parametric study.

A further study into the costs of the different components should be done to reduce the uncertainty.

A comparison between other different hybrid systems, storage technologies and different geographical locations should be done to see if and when CSP + PV with RO could be the best choice to drive desalination processes.

9 References

[1] World Data Lab, "Water Scarcity Clock," World Data Lab, 21 01 2019. [Online]. Available: https://worldwater.io/?utm_source=google&utm_medium=search&utm_campaign=Waterscarcityclock&campaignid=6444167483&adgroupid=75248439485&adid=376898575385&gclid=CjwKCAiA35rxBRAWEiwADqB375hqn0Y-TYvV6bZ0L5M9jlsdpFg_URLLQ-MQ7BT7JhVvMJlf7z7LMhoC12QQAvD_BwE. [Accessed 21 01 2019].

[2] WWF, "Allt jordens vatten i en liter," WWF, 19 08 2019. [Online]. Available: https://www.wwf.se/utbildning/uppgiftsbanken/jordens-vatten-i-en-liter/. [Accessed 20 01 2020].

[3] GWI, *Desalination Market Update,* GWI, 2020.

[4] A. Green, C. Diep, R. Dunn and J. Dent, "High capacity factor CSP-PV hybrid systems," *Energy Procedia,* vol. 69, pp. 2049-2059, 2015.

[5] M. Petrollese and D. Cocco, "Optimal design of a hybrid CSP-PV plant for achieving the full dispatchability of solar energy power plants," *Solar Energy,* vol. 137, pp. 477-489, 2016.

[6] W. Platzer, "PV-Enhanced Solar Thermal Power," *Energy Procedia,* vol. 57, pp. 477-486, 2014.

[7] A. Zurita, C. Mata-Torres, C. Valenzuela, C. Felbol, J. M. Cardemil, A. M. Guzmán and R. A. Escobar, "Techno-economic evaluation of a hybrid CSP + PV plant integrated with thermal energy storage and a large-scale battery energy storage system for base generation," *Solar Energy,* vol. 173, pp. 1262-1277, 2018.

[8] M. Laissoui, P. Palenzuela, M. A. Sharif Eldean, D. Nehari and D. C. Alarcón-Padilla, "Techno-economic analysis of a stand-alone solar desalination plant at variable load conditions," *Applied Thermal Engineering,* vol. 133, pp. 659-670, 2018.

[9] C. Valenzuela, C. Mata-Torres, J. M. Cardemil and R. A. Escobar, "CSP + PV hybrid solar plants for power and water cogeneration in northern Chile," *Solar Energy,* vol. 157, pp. 713-726, 2017.

[10] P. Palenzuela, D. C. Alarcón-Padilla and G. Zaragoza, Concetrating Solar Power and Desalination Plants: Engineering and Economics of Coupling Multi-Effect Distillation and Solar Plants, Springer, 2015.

[11] B. Ortega, P. Palenzuela, D. Alarcón and L. García, Theoretical analysis of high efficient multi-effect distillation processes and their integration into Concentrating Solar Power Plants, Madrid: CIEMAT, 2017.

[12] S. Burn and S. Gray, Efficient Desalination by Reverse Osmosis : A guide to RO practice, London: IWA Publishing, 2015.

[13] R. L. Stover, "Energy Recovery Device Performance Analysis," Water Middle East, 2005.

[14] M. Liu, S. N. Tay, S. Bell, M. Belusko, R. Jacob, G. Will, W. Saman and F. Bruno, "Review on concentrating solar power plants and new developments in high temperature thermal energy storage technologies," *Renewable and Sustainable Energy Reviews,* vol. 53, pp. 1411-1432, 2016.

[15] SunPower, "Products: Datasheets," September 2017. [Online]. Available: https://us.sunpower.com/sites/default/files/sunpower-x-series-commercial-solar-panels-x21-470-com-datasheet-524935-revb.pdf?fbclid=IwAR1Ynhcsg_wsav5J2Z0cCdTE5PChoa0F6QuXwmYFwHzxXYly-yWmpzK3E7w. [Accessed 18 March 2020].

[16] J. Kim, K. Park, D. R. Yang and S. Hong, "A comprehensive review of energy consumption of seawater reverse osmosis," *Applied Energy,* vol. 254, 2019.

[17] European Commission, "PHOTOVOLTAIC GEOGRAPHICAL INFORMATION SYSTEM," European Commission, 15 October 2019. [Online]. Available: https://re.jrc.ec.europa.eu/pvg_tools/en/tools.html#TMY. [Accessed 7 February 2020].

[18] A. B. Zavoico, "Solar Power Tower Design Basis Document, Revision 0," Sandia, San Francisco, 2001.

[19] European Investment Bank, "EIB Project Carbon Footprint Methologies: Methologies for the Assessment of Project GHG Emissions and Emission Variations," European Investment Bank, 2018.

[20] R. R. Kommalapati, A. Kadiyala, M. T. Shahriar and Z. Huque, "Review of the Life Cycle Greenhouse Gas Emissions from Different Photovoltaic and Concentrating Solar Power Electricity Generation Systems," *Energies,* vol. 10, p. 350, 2017.

[21] NREL, *System Advisor Model Help, CSP Power Rower, System Costs,* NREL, 2019.

[22] R. Fu, D. Feldman and R. Margolis, "U.S. Solar Photovoltaic System Cost Benchmark: Q1 2018," NREL, 2018.

[23] NREL, NREL, 03 june 2010. [Online]. Available: https://www.nrel.gov/analysis/tech-lcoe-documentation.html. [Accessed 3 March 2020].

[24] desaldata.com, "cost estimator," desaldata.com, [Online]. Available: https://www.desaldata.com/cost_estimator. [Accessed 03 March 2020].

[25] GlobalPetrolPrices.com, "Kuwait electricity prices," GlobalPetrolPrices.com, March 2020. [Online]. Available: https://www.globalpetrolprices.com/Kuwait/electricity_prices/. [Accessed 3 March 2020].

[26] European Commission, "Report on the functioning of the European carbon market," European Comission, Brussels, 2020.

[27] D. Alarcón and P. Palenzuela, *"Re: Cost of storage" Personal Email,* 2020.

Appendix A

This part presents the tables of all results from simulations. These were used when calculating the rest of the results.

Table A.1 Total energy generated, in GWh, for different PV size, SM and TES.

Total energy (GWh)	***TES (h)***	***PV (MW)***	*0*	*4*	*8*	*12*	*16*	*20*	*24*	*28*	*32*
no CSP	0		0	7	14	21	28	35	42	49	57
SM 2	2		51								
	4		57	61							
	6		59	65	69	72	75	80	82	86	92
	8		59	65	71	77	82	87	90	95	100
	10		59	65	71	78	85	91	96	102	108
	12				71	78	85	92	100	106	113
	14					78	85	92	100	108	115
	16							92	100	108	115
	18									108	115
SM 2.5	6		69	72	73	75	77	81	83	87	92
	8		73	77	80	83	86	90	92	96	102
	10		73	80	85	89	93	98	100	105	111
	12		73	80	86	92	98	103	107	113	118
	14		73	80	86	93	100	106	112	118	124
	16				86	93	100	107	113	119	125
	18					93	100	107	113	119	125
SM 3	10		85	88	91	93	96	100	102	107	112
	12		88	93	97	100	103	108	111	115	121
	14		88	95	100	105	109	114	117	122	128
	16		88	95	100	105	110	115	119	124	129
	18		88	95	101	106	111	116	120	124	130
	20				101	106	111	116	120	125	130
SM 3.5	12		96	99	102	103	106	110	112	117	122
	14		101	105	108	111	113	118	120	125	130
	16		102	106	109	112	115	120	122	127	132
	18		102	106	110	113	116	120	123	127	133
	20		102	107	110	113	116	121	123	128	133

Table A.2 Excess energy that is sold to the grid or discarded.

Excess energy (GWh)	***TES (h)***	***PV (MW)***	*0*	*4*	*8*	*12*	*16*	*20*	*24*	*28*	*32*
PV	0		0.00	0.00	0.00	0.00	0.00	0.11	2.21	6.24	11.16
SM 2	2		0.00								
	4		0.00	0.00							
	6		0.00	0.00	0.00	0.00	0.93	3.99	4.54	7.81	12.37
	8		0.00	0.00	0.00	0.00	0.93	3.98	4.53	7.79	12.34
	10		0.00	0.00	0.00	0.00	0.93	3.98	4.52	7.77	12.31
	12				0.00	0.00	0.93	3.97	4.51	7.76	12.28
	14					0.00	0.93	3.96	4.50	7.74	12.26
	16							3.96	4.50	7.72	12.23
	18									7.69	12.20
SM 2.5	6		0.00	0.00	0.00	0.00	0.93	3.99	4.56	7.83	12.39
	8		0.00	0.00	0.00	0.00	0.93	3.99	4.55	7.81	12.36
	10		0.00	0.00	0.00	0.00	0.93	3.98	4.54	7.79	12.34
	12		0.00	0.00	0.00	0.00	0.93	3.98	4.53	7.78	12.32
	14		0.00	0.00	0.00	0.00	0.93	3.97	4.52	7.77	12.31
	16				0.00	0.00	0.93	3.97	4.52	7.76	12.30
	18					0.00	0.93	3.97	4.51	7.75	12.30
SM 3	10		0.00	0.00	0.00	0.00	0.93	3.99	4.55	7.81	12.36
	12		0.00	0.00	0.00	0.00	0.93	3.98	4.54	7.79	12.34
	14		0.00	0.00	0.00	0.00	0.93	3.98	4.53	7.78	12.33
	16				0.00	0.00	0.93	3.98	4.53	7.79	12.35
	18		0.00	0.00	0.00	0.00	0.93	3.98	4.53	7.79	12.35
	20		0.00	0.00	0.00	0.00	0.93	3.98	4.53	7.78	12.34
SM 3.5	12		0.00	0.00	0.00	0.00	0.93	3.99	4.55	7.81	12.36
	14		0.00	0.00	0.00	0.00	0.93	3.98	4.54	7.80	12.35
	16		0.00	0.00	0.00	0.00	0.93	3.98	4.55	7.81	12.37
	18		0.00	0.00	0.00	0.00	0.93	3.99	4.55	7.81	12.38
	20		0.00	0.00	0.00	0.00	0.93	3.98	4.55	7.82	12.39

Table A.3 Deficit energy to be covered by the grid.

Deficit Energy (GWh)	***TES (h)***	***PV (MW)***	*0*	*4*	*8*	*12*	*16*	*20*	*24*	*28*	*32*
PV			124.8	117.8	110.7	103.6	96.6	89.6	84.6	81.6	79.4
SM 2	2		73.7								
	4		67.6	64.1							
	6		66.2	60.2	55.7	52.7	50.6	49.2	47.7	46.5	45.6
	8		66.2	59.7	53.6	48.0	44.1	42.0	39.6	37.9	36.7
	10		66.2	59.7	53.5	46.9	41.1	37.6	33.1	30.8	29.2
	12				53.5	46.9	40.7	36.5	29.7	26.2	24.1
	14					46.9	40.7	36.5	29.1	24.9	22.2
	16							36.5	29.0	24.8	22.1
	18									24.7	22.0
SM 2.5	6		55.9	53.3	51.5	49.9	48.6	47.6	46.6	45.6	44.8
	8		52.1	47.7	44.5	42.1	40.2	38.9	37.4	36.3	35.3
	10		51.4	45.1	40.1	36.1	33.0	31.3	29.2	27.6	26.5
	12		51.4	44.8	38.7	32.7	28.1	25.6	22.0	20.1	18.7
	14		51.4	44.9	38.6	32.0	26.1	22.5	17.3	14.8	13.3
	16				38.6	32.0	25.9	22.1	16.7	13.9	12.4
	18					32.0	25.9	22.0	16.4	13.6	12.0
SM 3	10		39.7	36.3	33.8	31.7	30.0	28.7	27.2	26.0	25.1
	12		37.0	31.9	28.1	24.9	22.4	20.8	18.9	17.4	16.3
	14		36.5	30.2	24.8	20.2	16.7	14.7	12.0	10.4	9.3
	16		36.4	30.0	24.4	19.4	15.6	13.5	10.5	8.8	7.8
	18		36.5	30.0	24.3	19.1	15.2	12.9	9.9	8.2	7.2
	20				24.2	18.9	14.9	12.5	9.5	7.9	6.9
SM 3.5	12		28.4	25.5	23.3	21.5	19.8	18.5	17.1	15.9	14.9
	14		24.1	20.1	17.0	14.4	12.4	11.1	9.4	8.1	7.2
	16		23.3	19.0	15.6	12.7	10.4	9.1	7.4	6.2	5.4
	18		23.0	18.5	15.0	12.1	9.7	8.5	6.6	5.4	4.6
	20		22.8	18.3	14.6	11.7	9.3	8.0	6.2	5.0	4.2

Appendix B

This part presents tables of all results from calculations.

Table B.1 CF of the CSP + PV plants for case b

CF b	***TES (h)***	***PV (MW)***	0	4	8	12	16	20	24	28	32
no CSP	0		0	0.05	0.11	0.16	0.22	0.27	0.31	0.33	0.35
SM 2	2		0.39								
	4		0.44	0.46							
	6		0.45	0.49	0.53	0.55	0.57	0.58	0.59	0.60	0.60
	8		0.45	0.50	0.54	0.58	0.61	0.63	0.65	0.66	0.67
	10		0.45	0.50	0.54	0.59	0.64	0.66	0.70	0.72	0.73
	12				0.54	0.59	0.64	0.67	0.72	0.75	0.77
	14					0.59	0.64	0.67	0.73	0.76	0.78
	16							0.67	0.73	0.76	0.78
	18									0.76	0.78
SM 2.5	6		0.52	0.54	0.56	0.57	0.58	0.59	0.60	0.60	0.61
	8		0.55	0.59	0.61	0.63	0.64	0.65	0.67	0.67	0.68
	10		0.56	0.61	0.65	0.68	0.70	0.71	0.73	0.74	0.75
	12		0.56	0.61	0.66	0.70	0.74	0.76	0.78	0.80	0.81
	14		0.56	0.61	0.66	0.71	0.75	0.78	0.82	0.84	0.85
	16				0.66	0.71	0.75	0.78	0.82	0.84	0.86
	18					0.71	0.75	0.78	0.83	0.85	0.86
SM 3	10		0.65	0.67	0.69	0.71	0.72	0.73	0.74	0.75	0.76
	12		0.67	0.71	0.74	0.76	0.78	0.79	0.81	0.82	0.83
	14		0.67	0.72	0.76	0.80	0.82	0.84	0.86	0.87	0.88
	16		0.67	0.72	0.76	0.80	0.83	0.85	0.87	0.88	0.89
	18		0.67	0.72	0.77	0.81	0.83	0.85	0.87	0.89	0.90
	20				0.77	0.81	0.84	0.86	0.88	0.89	0.90
SM 3.5	12		0.73	0.76	0.77	0.79	0.80	0.81	0.82	0.83	0.84
	14		0.77	0.80	0.82	0.84	0.86	0.87	0.88	0.89	0.90
	16		0.77	0.81	0.83	0.85	0.87	0.88	0.89	0.90	0.91
	18		0.77	0.81	0.84	0.86	0.88	0.89	0.90	0.91	0.91
	20		0.78	0.81	0.84	0.86	0.88	0.89	0.90	0.91	0.92

Table B.2 LCOE for case a.

LCOE a (USD/kWh)	***TES (h)***	***PV (MW)***	0	4	8	12	16	20	24	28	32
no CSP	0			0.046	0.046	0.046	0.046	0.046	0.046	0.046	0.046
SM 2	2		0.136								
	4		0.124	0.122							
	6		0.124	0.117	0.114	0.114	0.113	0.111	0.112	0.110	0.107
	8		0.126	0.119	0.113	0.109	0.106	0.104	0.104	0.102	0.099
	10		0.129	0.121	0.115	0.109	0.104	0.100	0.098	0.096	0.094
	12				0.117	0.111	0.106	0.101	0.097	0.094	0.091
	14					0.113	0.107	0.102	0.098	0.094	0.091
	16							0.104	0.099	0.095	0.092
	18									0.097	0.093
SM 2.5	6		0.116	0.117	0.118	0.119	0.120	0.118	0.119	0.117	0.114
	8		0.113	0.110	0.110	0.110	0.110	0.108	0.109	0.108	0.105
	10		0.114	0.109	0.106	0.105	0.104	0.102	0.102	0.100	0.098
			0.115	0.110	0.106	0.103	0.100	0.098	0.097	0.095	0.093
	14		0.118	0.112	0.108	0.103	0.100	0.096	0.094	0.092	0.090
	16				0.109	0.105	0.101	0.097	0.095	0.093	0.091
	18					0.107	0.102	0.099	0.096	0.094	0.092
SM 3	10		0.107	0.106	0.107	0.108	0.108	0.106	0.107	0.106	0.103
	12		0.106	0.103	0.102	0.102	0.102	0.100	0.101	0.099	0.097
	14		0.107	0.103	0.101	0.099	0.098	0.096	0.096	0.095	0.093
	16		0.108	0.104	0.102	0.100	0.098	0.097	0.096	0.095	0.093
	18		0.110	0.106	0.103	0.101	0.099	0.098	0.097	0.096	0.094
	20				0.104	0.102	0.100	0.098	0.098	0.097	0.095
SM 3.5	12		0.104	0.104	0.105	0.106	0.106	0.105	0.106	0.104	0.102
	14		0.101	0.100	0.100	0.101	0.101	0.100	0.101	0.099	0.098
	16		0.102	0.101	0.100	0.101	0.100	0.099	0.100	0.099	0.097
	18		0.103	0.102	0.101	0.101	0.101	0.100	0.101	0.100	0.098
	20		0.104	0.103	0.102	0.102	0.102	0.101	0.102	0.100	0.099

Table B.3 LCOE for case b.

LCOE b (USD/kWh)	***TES (h)***	***PV (MW)***	0	4	8	12	16	20	24	28	32
no CSP	0			0.046	0.046	0.046	0.046	0.046	0.048	0.052	0.057
SM 2	2		0.136								
	4		0.124	0.122							
	6		0.124	0.117	0.114	0.114	0.115	0.117	0.118	0.121	0.123
	8		0.126	0.119	0.113	0.109	0.108	0.109	0.109	0.111	0.113
	10		0.129	0.121	0.115	0.109	0.106	0.105	0.103	0.104	0.106
	12				0.117	0.111	0.107	0.105	0.101	0.101	0.102
	14					0.113	0.109	0.107	0.102	0.101	0.102
	16							0.109	0.104	0.102	0.103
	18									0.104	0.104
SM 2.5	6		0.116	0.117	0.118	0.119	0.121	0.124	0.126	0.129	0.131
	8		0.113	0.110	0.110	0.110	0.111	0.113	0.115	0.117	0.119
	10		0.114	0.109	0.106	0.105	0.105	0.106	0.107	0.108	0.110
	12		0.115	0.110	0.106	0.103	0.101	0.102	0.101	0.102	0.104
	14		0.118	0.112	0.108	0.103	0.100	0.100	0.098	0.099	0.100
	16				0.109	0.105	0.102	0.101	0.099	0.099	0.101
	18					0.107	0.103	0.102	0.100	0.100	0.102
SM 3	10		0.107	0.106	0.107	0.108	0.109	0.111	0.112	0.114	0.116
	12		0.106	0.103	0.102	0.102	0.103	0.104	0.105	0.107	0.108
	14		0.107	0.103	0.101	0.099	0.099	0.100	0.100	0.102	0.103
	16		0.108	0.104	0.102	0.100	0.099	0.100	0.100	0.102	0.103
	18		0.110	0.106	0.103	0.101	0.100	0.101	0.101	0.102	0.104
	20				0.104	0.102	0.101	0.102	0.102	0.103	0.105
SM 3.5	12		0.104	0.104	0.105	0.106	0.107	0.109	0.110	0.112	0.114
	14		0.101	0.100	0.100	0.101	0.102	0.103	0.104	0.106	0.108
	16		0.102	0.101	0.100	0.101	0.101	0.103	0.104	0.106	0.108
	18		0.103	0.102	0.101	0.101	0.102	0.104	0.104	0.106	0.108
	20		0.104	0.103	0.102	0.102	0.103	0.104	0.105	0.107	0.109

Table B.4 Solar fraction for system 1.

Solar fraction	***TES (h)***	***PV (MW)***	0	4	8	12	16	20	24	28	32
no CSP	0		0.00	0.06	0.11	0.17	0.23	0.28	0.32	0.35	0.36
SM 2	2		0.41	0.00	0.00	0.00	0.00	0.00	0.00	0.00	0.00
	4		0.46	0.49	0.00	0.00	0.00	0.00	0.00	0.00	0.00
	6		0.47	0.52	0.55	0.58	0.59	0.61	0.62	0.63	0.63
	8		0.47	0.52	0.57	0.62	0.65	0.66	0.68	0.70	0.71
	10		0.47	0.52	0.57	0.62	0.67	0.70	0.73	0.75	0.77
	12				0.57	0.62	0.67	0.71	0.76	0.79	0.81
	14					0.62	0.67	0.71	0.77	0.80	0.82
	16							0.71	0.77	0.80	0.82
	18									0.80	0.82
SM 2.5	6		0.55	0.57	0.59	0.60	0.61	0.62	0.63	0.63	0.64
	8		0.58	0.62	0.64	0.66	0.68	0.69	0.70	0.71	0.72
	10		0.59	0.64	0.68	0.71	0.74	0.75	0.77	0.78	0.79
	12		0.59	0.64	0.69	0.74	0.77	0.79	0.82	0.84	0.85
	14		0.59	0.64	0.69	0.74	0.79	0.82	0.86	0.88	0.89
	16				0.69	0.74	0.79	0.82	0.87	0.89	0.90
	18					0.74	0.79	0.82	0.87	0.89	0.90
SM 3	10		0.68	0.71	0.73	0.75	0.76	0.77	0.78	0.79	0.80
	12		0.70	0.74	0.77	0.80	0.82	0.83	0.85	0.86	0.87
	14		0.71	0.76	0.80	0.84	0.87	0.88	0.90	0.92	0.93
	16		0.71	0.76	0.80	0.84	0.88	0.89	0.92	0.93	0.94
	18		0.71	0.76	0.81	0.85	0.88	0.90	0.92	0.93	0.94
	20				0.81	0.85	0.88	0.90	0.92	0.94	0.94
SM 3.5	12		0.77	0.80	0.81	0.83	0.84	0.85	0.86	0.87	0.88
	14		0.81	0.84	0.86	0.89	0.90	0.91	0.92	0.93	0.94
	16		0.81	0.85	0.87	0.90	0.92	0.93	0.94	0.95	0.96
	18		0.82	0.85	0.88	0.90	0.92	0.93	0.95	0.96	0.96
	20		0.82	0.85	0.88	0.91	0.92	0.94	0.95	0.96	0.97

Table B.5 GWP for system 1, case a.

GWP a ***(gCO_2/m^3)***	***TES*** ***(h)***	***PV*** ***(MW)***	*0*	*4*	*8*	*12*	*16*	*20*	*24*	*28*	*32*
no CSP	0		3067	2911	2752	2594	2436	2278	2120	1963	1805
SM 2	2		1951								
	4		1817	1737							
	6		1787	1652	1551	1480	1411	1311	1262	1162	1038
	8		1787	1642	1504	1379	1271	1154	1086	975	846
	10		1788	1642	1502	1355	1203	1058	945	819	683
	12				1502	1355	1196	1035	869	720	572
	14					1355	1196	1034	856	690	531
	16							1033	856	689	527
	18									689	527
SM 2.5	6		1561	1501	1459	1421	1368	1275	1238	1142	1021
	8		1479	1378	1305	1250	1185	1086	1038	938	815
	10		1463	1323	1208	1118	1027	919	858	750	622
	12		1462	1317	1178	1045	921	795	702	584	452
	14		1463	1317	1176	1029	877	727	599	471	334
	16				1177	1029	872	719	585	451	314
	18					1028	871	716	579	444	306
SM 3	10		1208	1131	1071	1023	961	862	815	715	591
	12		1149	1035	948	874	795	691	633	526	399
	14		1137	996	875	771	672	557	482	373	247
	16		1136	992	866	753	647	530	450	339	213
	18		1137	992	863	747	637	517	437	326	201
	20				862	742	631	508	428	319	193
SM 3.5	12		960	893	843	799	738	640	593	493	369
	14		866	776	705	644	577	478	426	324	201
	16		849	751	674	608	534	434	381	281	160
	18		842	740	661	595	519	421	365	264	144
	20		839	735	651	584	510	411	355	254	133

Table B.6 GWP for case b.

GWP b ***(gCO_2/m^3)***	***TES*** ***(h)***	***PV*** ***(MW)***	0	4	8	12	16	20	24	28	32
no CSP	0		3067	2911	2752	2594	2436	2281	2175	2116	2079
SM 2	2		1951								
	4		1817	1737							
	6		1787	1652	1551	1480	1434	1409	1374	1354	1342
	8		1787	1642	1504	1379	1294	1252	1197	1167	1149
	10		1788	1642	1502	1355	1226	1156	1056	1010	985
	12				1502	1355	1219	1132	980	910	874
	14					1355	1219	1131	967	880	832
	16							1131	966	879	828
	18									878	827
SM 2.5	6		1561	1501	1459	1421	1391	1373	1350	1335	1326
	8		1479	1378	1305	1250	1208	1184	1150	1130	1119
	10		1463	1323	1208	1118	1050	1017	970	942	925
	12		1462	1317	1178	1045	944	893	813	776	755
	14		1463	1317	1176	1029	900	825	710	662	636
	16				1177	1029	895	816	696	642	617
	18					1028	894	814	690	634	608
SM 3	10		1208	1131	1071	1023	984	960	927	907	895
	12		1149	1035	948	874	818	789	745	717	702
	14		1137	996	875	771	695	655	593	564	550
	16		1136	992	866	753	670	628	561	530	516
	18		1137	992	863	747	660	615	548	517	504
	20				862	742	654	606	539	510	497
SM 3.5	12		960	893	843	799	761	738	705	685	673
	14		866	776	705	644	600	576	538	515	504
	16		849	751	674	608	557	532	493	472	464
	18		842	740	661	595	542	519	477	456	448
	20		839	735	651	584	533	509	466	447	438

Table B.7 LCOW for system 1, considering an electricity price of 0.05 USD/kWh for buying and 0.00 USD/kWh for selling. No costs for emissions are considered.

LCOW 1 (USD/m³)	***TES (h)***	***PV (MW)***	0	4	8	12	16	20	24	28	32
no CSP	0		0.649	0.649	0.648	0.646	0.646	0.645	0.647	0.653	0.660
SM 2	2		0.790								
	4		0.785	0.790							
	6		0.788	0.789	0.792	0.797	0.803	0.811	0.818	0.827	0.835
	8		0.793	0.793	0.793	0.794	0.798	0.805	0.811	0.819	0.827
	10		0.798	0.798	0.798	0.798	0.798	0.803	0.806	0.813	0.820
	12				0.802	0.802	0.803	0.806	0.806	0.811	0.818
	14					0.807	0.807	0.811	0.810	0.813	0.819
	16							0.816	0.814	0.818	0.824
	18									0.822	0.828
SM 2.5	6		0.796	0.802	0.809	0.816	0.824	0.832	0.840	0.849	0.858
	8		0.795	0.798	0.803	0.809	0.816	0.824	0.831	0.840	0.848
	10		0.799	0.799	0.801	0.805	0.810	0.817	0.824	0.831	0.840
	12		0.804	0.804	0.804	0.805	0.807	0.814	0.818	0.825	0.833
	14		0.808	0.808	0.808	0.808	0.809	0.814	0.816	0.822	0.830
	16				0.813	0.813	0.814	0.818	0.819	0.825	0.833
	18					0.818	0.818	0.822	0.824	0.829	0.837
SM 3	10		0.805	0.810	0.815	0.822	0.829	0.837	0.844	0.853	0.861
	12		0.806	0.808	0.812	0.816	0.822	0.830	0.837	0.844	0.853
	14		0.810	0.810	0.811	0.814	0.819	0.826	0.831	0.839	0.847
	16		0.814	0.814	0.815	0.818	0.822	0.828	0.834	0.841	0.850
	18		0.819	0.819	0.820	0.822	0.826	0.832	0.837	0.845	0.853
	20				0.825	0.826	0.830	0.836	0.841	0.849	0.858
SM 3.5	12		0.816	0.822	0.828	0.835	0.842	0.850	0.857	0.866	0.874
	14		0.815	0.818	0.823	0.829	0.836	0.844	0.851	0.859	0.867
	16		0.818	0.821	0.826	0.831	0.837	0.845	0.852	0.861	0.869
	18		0.822	0.825	0.830	0.835	0.841	0.849	0.856	0.864	0.873
	20		0.827	0.830	0.834	0.839	0.845	0.853	0.860	0.868	0.877

Table B.8 LCOW for a special case of system 2, where a single train RO system was assumed to follow the power production at a constant SEC. This was used for selecting the systems for the parametric study regarding the number of trains.

LCOW 2 spec. (USD/m³)	***TES (h)***	***PV (MW)***	0	4	8	12	16	20	24	28	32
no CSP	0			8.12	4.15	2.83	2.17	1.78	1.59	1.51	1.46
SM 2	2		1.64								
	4		1.48	1.41							
	6		1.45	1.34	1.27	1.23	1.21	1.21	1.20	1.20	1.20
	8		1.46	1.34	1.24	1.17	1.13	1.11	1.09	1.09	1.09
	10		1.47	1.35	1.25	1.16	1.09	1.06	1.03	1.01	1.01
	12				1.25	1.16	1.09	1.06	0.99	0.97	0.97
	14					1.17	1.10	1.06	0.99	0.97	0.95
	16							1.07	1.00	0.97	0.96
	18									0.98	0.96
SM 2.5	6		1.28	1.25	1.24	1.23	1.22	1.22	1.22	1.22	1.23
	8		1.22	1.17	1.14	1.12	1.11	1.11	1.10	1.10	1.10
	10		1.22	1.14	1.09	1.05	1.03	1.02	1.01	1.01	1.01
	12		1.23	1.14	1.07	1.02	0.98	0.97	0.95	0.94	0.94
	14		1.23	1.15	1.08	1.02	0.97	0.95	0.91	0.91	0.90
	16				1.09	1.02	0.97	0.95	0.91	0.90	0.90
	18					1.03	0.98	0.96	0.92	0.91	0.90
SM 3	10		1.09	1.06	1.04	1.03	1.03	1.03	1.02	1.02	1.03
	12		1.06	1.02	0.99	0.97	0.96	0.96	0.95	0.95	0.95
	14		1.06	1.00	0.96	0.93	0.91	0.91	0.90	0.90	0.90
	16		1.07	1.01	0.97	0.93	0.91	0.90	0.89	0.89	0.89
	18		1.07	1.01	0.97	0.93	0.91	0.91	0.89	0.89	0.89
	20				0.97	0.94	0.92	0.91	0.89	0.89	0.90
SM 3.5	12		1.00	0.98	0.97	0.97	0.96	0.96	0.96	0.96	0.97
	14		0.96	0.94	0.92	0.91	0.91	0.91	0.90	0.90	0.91
	16		0.96	0.93	0.92	0.90	0.90	0.90	0.89	0.89	0.90
	18		0.96	0.93	0.92	0.90	0.90	0.90	0.89	0.89	0.90
	20		0.97	0.94	0.92	0.90	0.90	0.90	0.89	0.90	0.90